DESIGN OF RELOCATABLE MICROGRID FOR MILITARY APPLICATIONS

A Project Report

submitted by

ABHISHEK KUMAR

in partial fulfilment of the requirements

for the award of the Degree of

MASTER OF TECHNOLOGY

DEPARTMENT OF ELECTRICAL ENGINEERING

INDIAN INSTITUTE OF TECHNOLOGY MADRAS

MAY 2019

THESIS CERTIFICATE

This is to certify that the thesis entitled" **DESIGN OF RELOCATABLE MICROGRID FOR MILITARY APPLICATIONS**", submitted by **Abhishek Kumar** (EE17M011), to the Indian Institute of Technology (Madras), is a bonafide record of the research work done by him under my supervision. The contents of this thesis, in full or in parts, have not been submitted to any other Institute or University for the award of any degree or diploma. Any data, figure, analysis or text drawn from other sources have been appropriately cited in the references page.

Dr. Mahesh Kumar
Project Guide
Professor
Dept. of Electrical Engineering
IIT Madras, Pin-600036

Place: Chennai
Date: May 2019

ACKNOWLEDGEMENTS

I would like to express my sincere gratitude to my mentor and guide Prof. Mahesh Kumar for his invaluable guidance and constant support for steering me to a logical conclusion for my MTech project. His directions helped me identify the problem statement in detail and present the expected solution. I am indebted to him for the facilities extended to my efforts in the Power Quality and Automation Laboratory, ESB 342, Department of Electrical Engineering which facilitated timely execution of the desired simulations in an orderly sequence.

On this occasion I also express my heartfelt gratitude to my fellow researchers and colleagues who were a source of motivation and selfless assistance through the course of my project. My association with my fellow mates in the Power Quality and Simulation Laboratory for the project has set a strong foundation for me to work further in the field and execute projects on ground with utmost dedication true to the spirit of our Laboratory. In this context I would like to thank Shrikanth Kotra, Nafih Muhammad, N Pruthvi Chaitanya, Sathish, Hariharan, Lokesh N and Durga Malleswar Rao who shall continue to be the motivational elements in our common field of interest. Their patience and tireless participation in discussions for my project helped me evolve a better understanding of the subject as a whole.

At the end I must acknowledge the countless blessings and faith of my parents in me that kept me focused to realise my dream and present my first little endeavour in the field of Power System as it applies to military applications.

ABSTRACT

KEYWORDS: Charge Equalisation Circuit (CEC); DC-DC Converters; Engineer task Force (ETF); Maximum Power Point Tracking (MPPT); Renewable Energy (RE)

The Corps of Engineers with its motto of "Sarvatra" forms the most potent arm for the build up and execution of any operation in the Indian Army. Towards the furtherance of the Commander's plan an Engineer Task Force (ETF) performs a variety of mobility, counter mobility and survivability tasks. The need for reliable electric supply has been the backbone of all such tasks and is seen to expand as the world enters into the "Green Earth" concept. Further, in present scenario wherein we as a nation are still largely dependant on Gulf nations for fossil fuels, the sustenance if not the initiative for any military operation gets shadowed by the dependence on those nations. Another glaring feature in the recent days is the probability of FOL dumps being targeted by fidayeen groups as the latest modus operandi of such anti-national elements.

With wide range proliferation of renewable energy platforms and in specific PV, the onus to replace diesel generator sets to establish PV based DC or AC grids forms the prime thought of essence from the point of economy as well. The evolution of DC-DC, DC-AC converters present ample opportunity to apply them duly optimizing the operation of PV modules applying the concept of MPPT.

With this as the motivation, this study has been carried out to establish a small scale relocatable microgrid for military applications. The study proposes use of regular service vehicles to house all the necessary components of the microgrid for supplying power to isolated loads of surveillance centres, water points or Unit HQs. The charge equalisation circuit proposed ensures utilisation of resources available in house. Probably this shall be the one of the most economical yet environment friendly application in the military paraphernalia for long.

Contents

List of Figures

List of Tables

Chapter 1

INTRODUCTION

1.1 Relevance of Electrical Energy in Army

The Indian Army is designed to operate in independant, self contained mode in extreme climate, unfriendly terrain and extended periods of uncertainties. As a part of the ongoing modernisation program we have kept our pace matched to induct the state of art arms, weapons, surveillance and communication equipments and provide them to the grass root level at of tactical units and formations. This has naturally enhanced our demand for reliable and secure power sources to operate flawlessly. While diesel generators and batteries have offered themselves as source of power, their application is restricted to small clusters and require massive space for stocking of fuel which itself poses as a target for sabotage or enemy threat in hostile environment. Lead acid batterys on the other hand have so far proven to be uneconomical as a power source for its dependence on main grid for recharging.

As observed by the Central Electricity Regulatory Commission (CERC) and reflected in Fig. 1.1, it is envisaged that the trend of dipping rates of solar power since 2013-14 shall continue. Like many other fields, the defence sector also has wide scope for incorporating PV power as the mainstream source in the years to come. The availability of adequate real estate, and the operational need for quick installation and de-installation of microgrids for matching mobility of advancing columns offer convincing reasons for *The Corps of Engineers* to spearhead the pace of introducing solar power as the prime source of power.

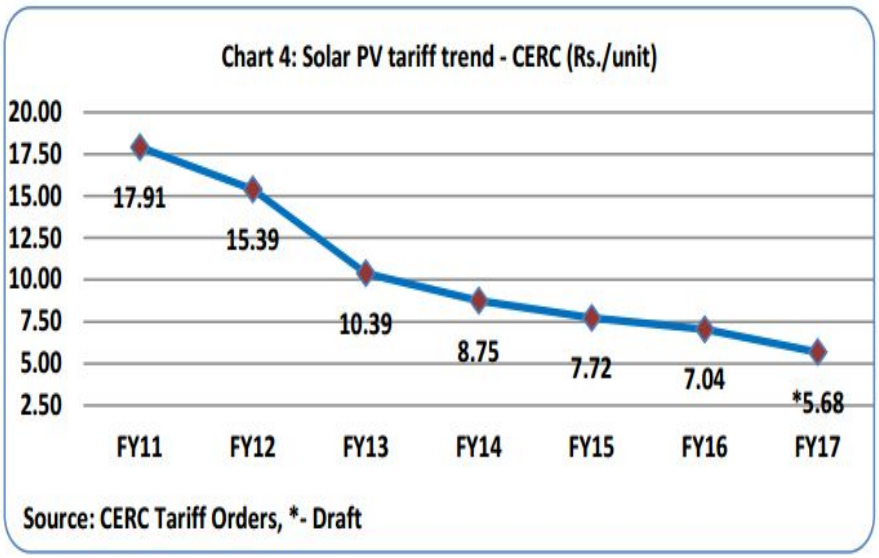

Figure 1.1: Dipping rates of PV since 2013

1.2 The Present Scenario

As on date the Indian Army has mighty dependence on the fossil fuels like diesel (DHPP-A), petrol (MT-87) and kerosene for propulsion of armoured tanks, heavy vehicles, gun towing vehicles, air crafts and a range of softer vehicles. Similarly, for the operation of several radar and surveillance centres we depend on diesel generators ranging from 2 kVA-63 kVA, when grid power supply is not available.

All this takes a remarkable toll of approx Rs 7000 Crores (as in FY 2016-17). While efforts have been initiated to establish a PV based source for night lamps or lamp posts with limited usage or criticality, yet the scope to craft and design a full fledged, versatile and mobile power generation and utilisation system that is tailor made for operational and peace time requirement remains unprobed to the required extent. A variety of equipments consume considerable amount of energy and if replenished from solar power can offer huge savings and security e.g. The Long-Range Reconnaissance and Observation System (LORROS) is a battle field surveillance radar that consumes approx 700 W and is operated on a 24 V battery set. Similarly, the counter mortar or artillery battery radar ANTPQ operates on a 43 kVA diesel generator.

While batteries are mostly employed for initial ignition, the scope to include the same as a mainstream source during off sun hours using the stored solar energy is worth examining and implementing. The amalgamation of these batterys serving as buffer for the PV source interfaced with power converter presents an excellent solution to cut the logistic chain in operational/ exercise scenario.

1.3 Solar Microgrid A Force Multiplier

The battle zone in a conventional warfare or even in counterinsurgency infested areas is dominantly dependant on the equipments which are electrically operated. A variety of specialised agencies or regiments are designed for electronic surveillance employing ANTPQ-37, LORROS and battle field surveillance radars (BFSRs). All these equipments depend on a reliable power source and need to be operating 24 x 7 as a critical operational requirement. Similarly Engineer Regiments at all levels of HQs are entrusted with task of providing a reliable power supply for the routine functioning of the Headquarter. Water supply for the troops' habitat and medical centres is another inevitable task during operations that calls for uninterrupted power supply.

Mobile, low weight quick to assemble setup of microgrid for such operational units shall reduce the turnaround time for the replenishment groups (RPGs) and enhance the potency of the offensive units to launch the final attack from their launchpads from their launchpads. Undoubtedly the reliability and security of the power source remain the critical parameter for employing it. However, the newly developed mono crystalline PV panels that can operate with better efficiencies even on cloudy days, robust Battery Energy and Storage Systems (BESS) and appropriate converters offer promising solution to start with.

The study undertakes a rigorous evaluation of load for an Engineer Task Force deployed for a given task and certain set of loads as in Table 2.1. A detailed study has been carried out to design a suitable PV based DC -DC microgrid for the area of consideration being Barmer sector of Rajasthan where the objective is to operate in isolated areas as an in-dependant, versatile, flexible and low cost solution for military operations. The template may be applied to any other area like Ladakh or Leh which may offer itself as a suitable ground for harnessing energy for military applications. Necessary amendments in terms of selecting the suitable panel based on insolation, temperature, reflective index and load profile should be undertaken by the user.

1.4 RE Applicable for Military Operations

1.4.1 Solar Energy

The location of India in the tropical belt has proven to be a boon for harnessing solar energy and replace the bio fossil fuels in the sector of industries, transport and many other promising applications. While all these entities may demand a huge investment ab-initio for acquiring real

estate and set up high density of battery charging infrastructure especially for electric vehicles, the application of the same in military environment has limited investment requirements for real estate as most of the operations would be mobile in nature. Thus the requirement of a dedicated real estate is avoidable; a vehicle mounted PV array suffices.

Military operations are invariably carried out in uninhabited areas where the availability of real estate is seldom an issue. As a matter of advantage, most of the operational fronts like Rajasthan, Punjab on Western front and Leh, Ladakh, Kargil on the Northern front experience solar insolation of approximately 5 kWh/m^2/day or above (ref Fig 1.2) [7]. A new record has been set in Bhadla, Rajasthan where the operation of solar power system has seen a per unit cost of Rs 2.44 only [11].

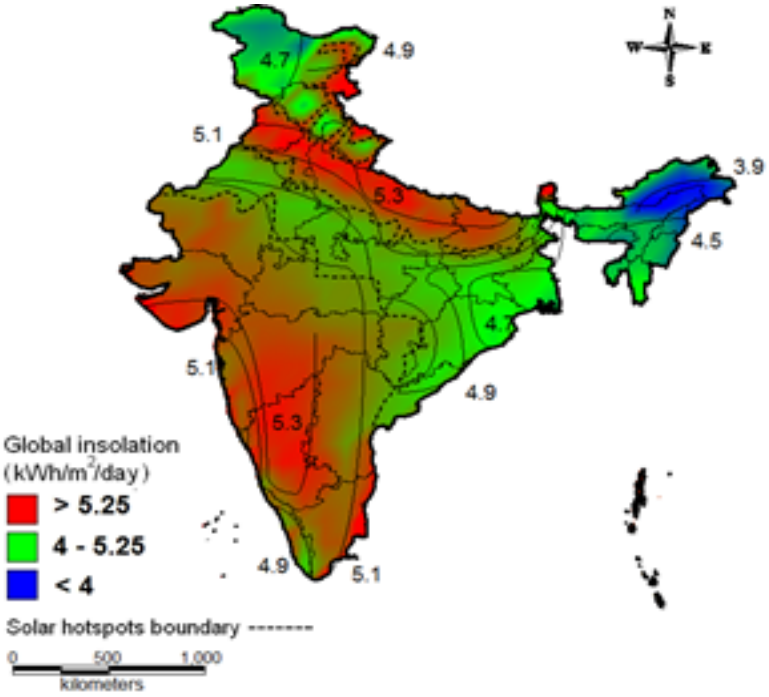

Figure 1.2: Average insolation over India

1.4.2 Wind Energy

Till 2013 when the cost of PV cells started reducing causing an accelerated growth in production and advanced research in photo voltaic systems, wind was the leading growing sector in the class of renewable energy. Places like Barmer, Jaisalmer, Kishangarh and Tanot have witnessed a series of wind mills installed to harness the free flowing winds over the vast stretches of barren dunes. Similarly, the coastlines have also attracted many companies to invest for harnessing the wind energy.

1.4.3 Mini Hydel Power

A large number of operational areas of the Indian Army are interspersed with a prominent network of rivers and its tributaries. While earlier they were seen as obstacles to be negotiated with heavy weight bridges, the concept of mini hydel power plants has revamped the perception of these water bodies and elevated their roles as potent power sources. Shyok River in Ladakh, Ganga in Joshimath and Brahmaputra and Teesta Rivers in North East and West Bengal are examples which have immense potential for serving as perennial source of power for the military habitats in such arduous terrains.

1.4.4 Tidal Power

The Indian coastline running upto 7517 km has immense potential for harnessing electricity through the tidal energy. For the tri-service establishments and in particular the naval, coast guard units and dockyards this could be a game changing solution once exploited in a bigger scale and dimension. The tidal energy is obtained from the effect of gravitational forces of the sun and the moon on the earth's water bodies. La Rance Tidal power station in France was the first such station the world and was set up as early as 1966. In India, the Gulf of Khambat, Gulf of Kutch and the delta regions of Sunderban seem to have prospects of tidal power plants in future with average tide height of 6.77 m , 5.23 m and 2.97 m respectively. According to the estimates of the Indian government, the country has a potential of 8,000 MW of tidal energy. This includes about 7,000 MW in the Gulf of Khambat in Gujarat, 1,200 MW in the Gulf of Kutch and 100 MW in the Gangetic delta in the Sunderbans region of West Bengal. With the naval and coast guard operational units and formations mostly deployed in and around the coastline, this form of power shall especially benefit them in a huge way.

1.4.5 Water Current

Inland Water Transport units of the Army are best suited to exploit the river current potential for storage and actively using suitable in regenerative modes. The ferrying and IWT units could clock huge saving on economy and also ensure a pollution free river bed on this account.

1.4.6 Tactical Considerations in Support of PV for Military Operations

While each of the above mentioned energy sources have their own features and challenges to generate electricity, solar power as on date suits the most for mobile military operations launched from semi permanent/ temporary bases of formation headquarters (HQs). The following reasons were examined and found true to incorporate PV source as mainstream power source.

1. Retrievable and Relocatable.
2. Rich insolation in most of the regions in India owing to our tropical location.
3. Vast expense of uninhabited areas available for installation during operations/ exercises.
4. Insolation range varying in the range of 5 kWh/ m^2/ day to 6 kWh/ m^2/ day in most of the operational fronts like North and North West India, which is optimally suited for the most efficient operation of PV panels. (Ref Fig 1.2)
5. The PVs can be used in conjunct with wind turbines for enhanced capacity as well as for cooling the panels.
6. DC-DC and DC -AC converters based on power electronic elements with higher efficiency and control features.
7. Competitive rates of PV arrays with enhanced adaptability to climatic conditions.

1.5 Research Motivation

The increasing influx of power steered equipments confirming to digitisation or automation in Army has also increased the dependence of Armed forces on bio fuels. The issue assumes greater significance during military operations where such dependence on bio fuels and hence on other nations is likely to overshadow our initiative and retard our advance. Apart from this, in the given scenario where fuel dumps in military areas are one of the most probable targets for the anti national elements it becomes necessary to replace them with secured renewable power sources. PV arrays clubbed with battery energy storage system (BESS) form the prime choice for such a requirement, thus promising a reliable and secure power source.

1.6 Aim of the Study

The study has been designed with the aim to provide a reliable power source for an Engineer Task Force in support of a small unit HQ with a certain set of load and predefined load curve. In this regards solar power using appropriate solar array is proposed. The array is designed for it to capture power for operating the load during the day and night. The BESS is designed and operated to store adequate power for the non insolation hours. Further, it has a smart logic to act as a source during deficit insolation (Mode I(a) and I(b)) and to act as a power sink for the solar array to allow operation at MPPT during excessive solar power (Mode II(a) and II(b)). The battery bank can be a single heavy duty bank commercially designed or even assembled in house using the charge equalisation circuits (CEC). The overall study was covered in the following phases.

- Acquiring load details, details of service vehicle dimensions and the battery specifications.
- Evaluation of the size of PV array required in accordance with given load variation and climatic conditions of temperature and insolation on curve for the given area.
- Validation of charge equalisation circuit using three batteries.
- Validation of the said scheme in MATLAB for various modes.

1.7 Organisation of Thesis

The thesis has been divided into six chapters as stated below.

Chapter 1 This chapter covers in detail the existing loads for which the relocatable microgrid (RMG) has been designed. A sample daily load curve is taken for evaluation of the requisite parameters. The details and specifications of service vehicles and batteries are also mentioned.
Chapter 2 The size of PV array required, battery sizing and the space/ real estate requirement for the said set up has been evaluated in this chapter.
Chapter 3 A summary on the concept of Maximum Power Point Tracking (MPPT) has been presented here and the various possible schemes including the incremental conductance MPPT on which this particular scheme has been implemented.
Chapter 4 discusses the design of the controllers for the different converters in the system. The controllers for the MPPT converter, bi-directional converters and the buck converter are designed using the frequency response of the converters.
Chapter 5 considers the operation of the scheme under various possible modes and evaluates the simulation results, that prove the credibility of the scheme in varying conditions of temperature, load and insolation.
Chapter 6 brings out the conclusion and scope of future enhancement in the same scheme, considering the requirements and terms of reference of military applications.

1.8 Summary

The need for clean and green energy can't be overemphasized. For military applications the reliability, security and economy are the primary requirements. There are a variety of renewable energy sources recognised in the world. Amongst them, solar and wind continue to be the major contributors of the total RE harnessed as on date. For military applications mini hydel power plants, tidal energy and water current also seem promising and may possibly find enhanced applications in the times to come.

In this study, the scope has been restricted to harnessing solar energy for establishing a mobile power source that suits the operational requirement of forces. A RMG could be configured using the knowledge of photovoltaics and power electronics to offer reliable, secure yet economical scheme in the existing trend of dropping price of solar panels and solar energy. While India as a nation has a geographical advantage in terms of insolation and irradiance, the mil-

itary applications do not require real estate to be permanently committed. Hence, it has been proposed in this study to use solar panels as roof tops for the service vehicles thus utilising the space as well as the mobility factor of these vehicles.

Apart from this it can be seen in the succeeding chapters that the battery bank used in the study can be assembled in house with charge equalisation circuit which further enhances the life of the batteries. Thus this project study is a complete solution for any service unit to form its mobile power source, better termed as Relocatable Micro Grid (RMG).

Chapter 2

Structure of the DC-DC Microgrid

2.1 Components of Solar Microgrid

The above mentioned configuration as in Fig 2.1 is a simple yet reliable scheme with integral control for the converters. The configuration is designed to be loaded and even set up comfortably on an Ashok Leyland Stallion or heavy mobility vehicle (HMV) like TATRA/ KRAZ. The setup basically is a power source, with converters for the required output and control requirement. The RMG is represented in the following diagrams.

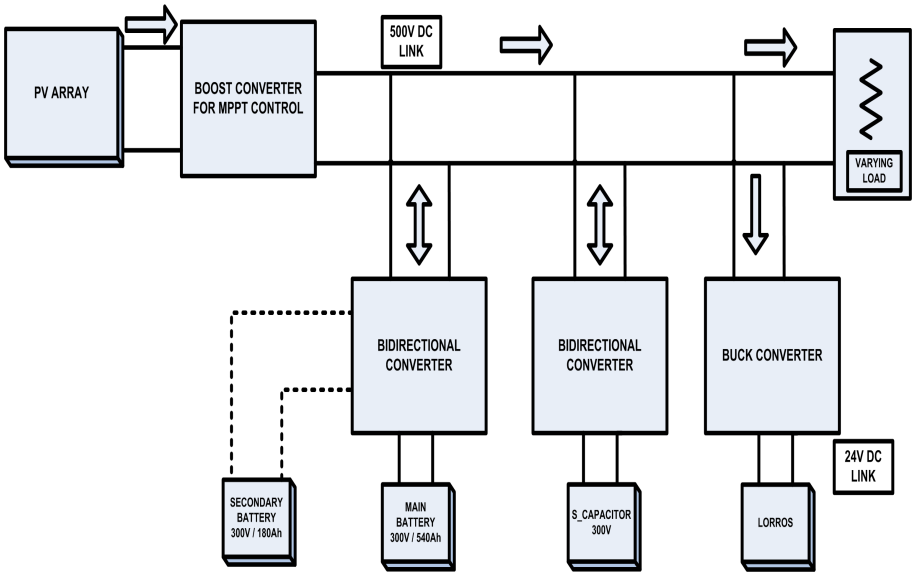

Figure 2.1: Schematic layout of relocatable microgrid

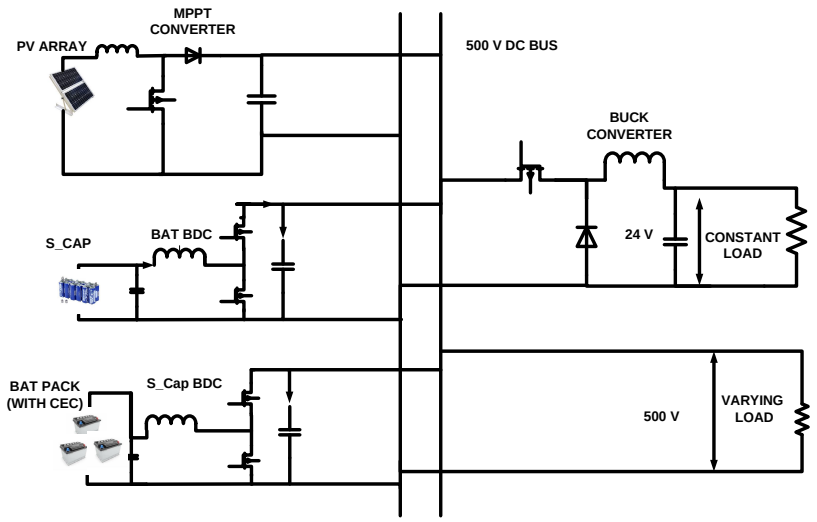

Figure 2.2: Circuit Diagram of relocatable microgrid

The block components of the system are listed below.

1. PV array 16.25 m x 10.19 m (165.6 m^2) over 12 TATRAs or 14 ALS as roof tops.
2. MPPT boost converter
3. MPPT controller
4. 300 V, 540 Ah lead acid battery bank with bi-directional converter (BDC)
5. Charge equalisation circuit
6. 300 V, 180 Ah lead acid battery
7. 84 F super capacitor with BDC
8. Buck converter for 24 V output
9. Loads at 500 V bus and 24 V bus

2.2 PV Module

A PV module is a combination of multiple PV cells arranged and connected to give a required output voltage or current when subjected to sunlight. The PV module is so selected that it renders adequate power irrespective of the moderately overcast weather. A mono crystalline PV cell is best suited for all terrain military applications. A typical PV cell can be modelled as

a pn junction source which acts as a current source when excited by light of suitable wavelength. As light falls on the junction which is designed to be highly doped and thin, electron hole pairs (EHP) are formed in the depletion region. The electrons so formed accumulate in the n region while the holes are accumulated in abundance in the p region. This entails a potential difference between between the two regions which when connected through a load allows the flow of photo voltaic current in the load. For varying wavelength the PV cell shall absorb a different amount of photon energy and accordingly a variable current is expected to flow. Fig. 2.3 (a) illustrates the model of a PV cell which acts as a current source across a pn junction diode with a shunt and a series resistance as depicted. The IV curve for a typical PV cell is shown in Fig. 2.3 (b)

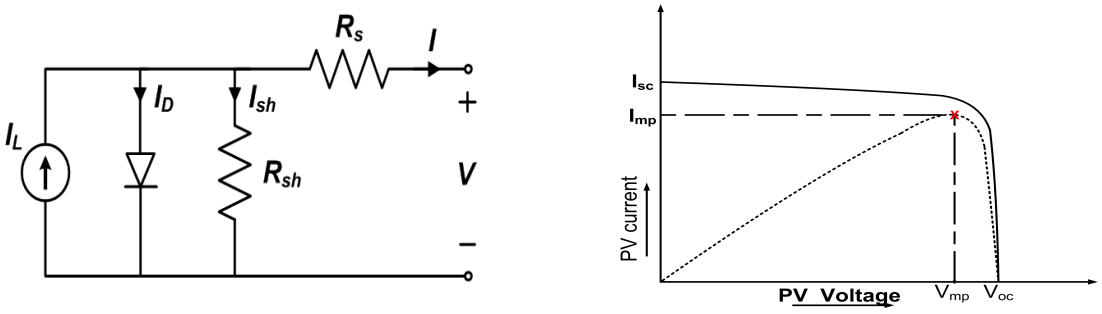

(a) PV cell-equivalent diagram

(b) IV curve

Figure 2.3: Solar cell characteristics

As seen in the equivalent circuit diagram, the Kirchhoff's current law gives the following equations.

$$I_l = I_d + I_{sh} + I$$

$$I = I_l - I_d - I_{sh}$$

$$I = I_l - I_d - \frac{(V + IR_s)}{R_{sh}}$$

$$I = I_l - I_o(e^{\frac{V+IR_s}{nV_T}} - 1) - \frac{(V + IR_s)}{R_{sh}} \tag{2.1}$$

where,

$I_o =$ reverse saturation current

$n = 2$ for silicon

$V_T = T/11600$

$K =$constant

$V_{G_O} =$ forbidden gap energy in eV

$T =$ temperature in K

The values of I_{sc} and V_{oc} can be determined from the above equations using the special conditions i.e. For a short circuit current to flow the terminal voltage is zero (V=0) and in open circuit condition the current flowing through the PV cell is zero (I=0). Substituting the desired conditions in Eq 2.1, the short circuit current and the open circuit voltages are evaluated in succeeding sections.

I_{sc} and V_{oc} Calculations

Substituting V = 0 , $I = I_{sc}$ and considering the fact that Rs« Rsh the Eqn 2.1 is summarised as $I_{SC} = I_l$. Substituting $V = V_{oc}$, I=0 and considering the fact that Voc« Rsh the Eqn, 2.1 is summarised as $V_{OC} = nV_T ln\frac{I_l+I_o}{I_o}$. The general equation for a PV array can be written as follows.

$$I = N_p I_l - N_p I_s[e^{\frac{V/N_s+IR_S/N_p}{nV_T}} - 1] - (\frac{N_p V}{N_s R_{sh}} + \frac{IR_s}{R_{sh}})$$

2.3 Design of PV Array

A typical military set up in operational scenario is likely to have a variety of loads viz. the operational (critical) loads, the office/ HQs pattern loads and the logistic echelon loads. A similar load pattern has been exhibited here. The load curve may vary for different military installations depending upon the specific role of that installation. The design for any power system setup is primarily based on the load demand through the day.

2.3.1 Load Details and Load Curve

The electrical load considered for the project depicts an ETF deployed in deserts in support of a HQ, with operations briefing room, office staff, communication centre, surveillance centre, field troops and a workshop. The load summary in the 24 hr cycle with cumulative energy demand for day and night is given at Table 2.1.

2.3.2 Calculations for Array Sizing

Based on the load curve in Fig. 2.4, the overall energy demand can be evaluated. The PV array along with battery energy storage system (BESS) must not only cater for the peak load in the day but also for that at night, condition to the availability of PV. Also it must be able to operate at the maximum power point of the array using the MPPT algorithm. This shall ensure full

Table 2.1: Load description for the study

S. no	Description	Qty	Eq Wattage	Dur Day	Dur Night	Daytime kWh	Ni time kWh
1.	LORROS	1	696	10	14	6960	9744
2.	Pumps	2	380	4	1	3040	760
3.	Telephone Exch	2	180	10	14	3600	5040
4.	Computers	8	250	5	1	10000	500
5.	Coolers	10	562.5	(7+1)	1	22500	1125
6.	Tube Light	20	50	7	1	7000	250
7.	AC 1.5TON	2	1500	(7+1)	0	12000	0
8.	Fans Pedestal	7	125	0	1	0	875
9.	Projectors	1	312.5	2	0	625	0
10.	Workshop	1	1100	3	0	3300	0
11.	CFL 15W	4	18.75	0	12	0	900
12.	CFL 11W	8	13.75	0	3	0	330
13.	Fans	20	62.5	0	7	0	8750
14.	Cooking Blowers	2	250	2	4	1000	2000

utilisation of the array. The size of the array can be decided based on the parameters stated below.

1. Day load (Wh_{day})
2. Night load (Wh_{ni}/η_B)
3. Autonomous operation of load for say n_a days and n_r days for recharging the battery.

A summary of the important load parameters for the proposed PV system is as at Table 2.2. If Wh_{pv} is the energy that a the PV array must capture through a day, it can be summed up as:-

$$Wh_{pv} = Wh_{day} + \frac{Wh_{ni}}{\eta_B} + \frac{Wh_{day} + Wh_{ni}}{\eta_B} . \frac{n_a}{n_r}$$

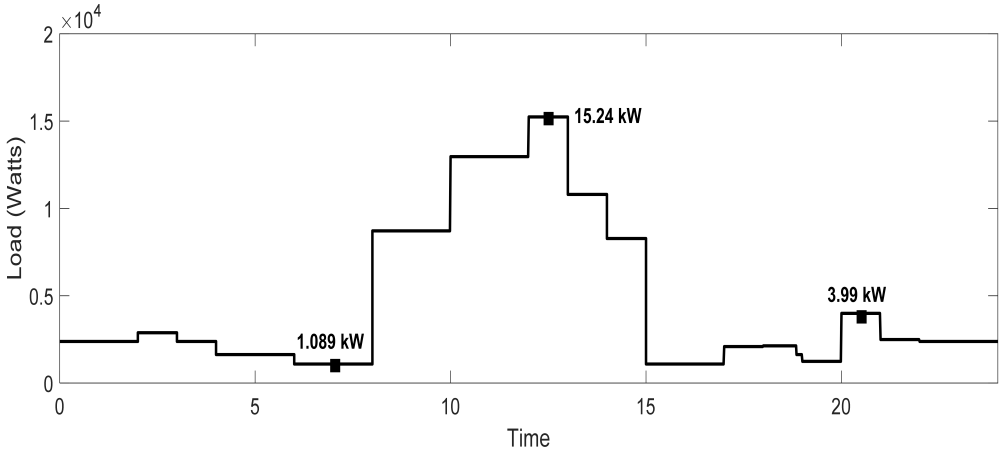

Figure 2.4: Daily load curve for the military application

.

Table 2.2: Essential load parameters

Sno	Load parameters	Values	Remarks
1	All day peak load	15.24 kW	Ideally supplied by PV
2	Ni time peak load	3.99 kW	Supplied by battery only
3	Daytime energy demand	85.193 kWh	Load + battery charging PV
4	Night time energy demand	27.08 kWh	Supplied by battery
5	All day peak load current	30.48 A	Battery designed to cater
6	Night time load current	7.98 A	Supplied by battery

For our project study we have considered Barmer as a location and assumed $n_a = n_r = 0$ given that it is unlikely for the location to see a complete day of inadequate insolation. However, necessary amendments can always be undertaken for the a situation wherein the above mentioned condition is not true. The size of the PV array and the battery size shall accordingly increase. Based on the load curve in Fig. 2.4 the (Wh_{day}) and (Wh_{ni}) are 85.193 kWh and 27.08 kWh respectively. Considering the battery efficiency as (η_B) ,

$$Wh_{pv} = Wh_{day} + \frac{Wh_{ni}}{\eta_B}$$

The peak array power assuming the $H_{at_{min}} = 5$ for Barmer would be

$$P_m = \frac{Wh_{pv}}{5}$$

$$= \frac{85.193 + \frac{27.08}{.7}}{5} = 24.78 \approx 25kW$$

The available service vehicles in the Indian Army that can be probably used to form the carrier vehicle for the said relocatable microgrid are listed below. Depending upon the net electrical load, terrain and the vehicle loading capability one of the vehicles mentioned in the table below could be selected.

Table 2.3: Service vehicles with dimensions of carrier

Vehicle	Length (m)	Height (m)	Width (m)	Weight (kg)
2.5 Ton	4	1.62	2.16	5150
ALS	4.7	1.64	2.5	6880
TATRA 8x8	5.5	1.69	2.5	13700
TATRA 6x6	5.4	1.67	2.5	12800
TATRA 4X4	5.2	1.65	2.5	12000

For a peak load of 15.24 kW and 24 hr consumption 25 kWh is to be planned using the panel selected with specifications as at Table 2.4. It is evaluated that to maintain the desired PV voltage, a set of 10 PV modules in series needs to be created. Each of 10 such sets shall be connected in parallel to achieve the desired current that serves the daytime load as well as the charging of the battery and super capacitor set. This shall amount to a total of 100 modules.

Based on the dimensions of the vehicle carrier of the vehicles mentioned at Table 2.3, one TATRA 8x8 shall suffice to carry the PV load. Apart from that, the vehicle (say TATRA) shall have a set of nine batteries each 100 V, 180 Ah as a part of the RMG. The PV modules selected for the design of RMG is of Mitsubishi make and has the following specifications.

Table 2.4: Specifications of Mitsubishi PV-MLU255HC

Sno	Specification	Value
1.	Isc	8.89 A
2.	Voc	37.8 V
3.	Imp	8.18 A
4.	Vmp	31.2 A
5.	Pmp	255 Wp

2.4 Control of the PV array

A PV array by virtue of its characteristic curve (Ref Fig. 4.8 and Fig. 4.9) has a property to be operated in a wide range of voltage and current. Thus for any given insolation and temperature any PV array can be controlled to operate at it's maximum power point which shall require the maximum power point tracking (MPPT) techniques. This however shall require a energy storage device like a battery, flywheel, super capacitor to act as a buffer for the surplus or deficit power that is generated viz a viz the instantaneous load.

2.5 Design of Battery Bank

2.5.1 Battery Specifications

The main battery considered must have a nominal voltage such that the BDC is not over-tasked i.e. duty of the BDC during the boost operation must not exceed 0.5. Hence, the battery of 300 V is planned. Further, the off insolation hours energy demand of 27.08 kWh must be handled by the battery capacity assuming that it gets charged fully during the insolation hours. Similarly, the secondary battery must also have a nominal voltage of 300 V. It could however be of a smaller capacity depending upon the primary task that it is employed for. The capacity of the primary battery is evaluated as below.

$$Wh_{load} = \frac{Wh_{ni}}{\eta_B} = \frac{27.08}{0.7} = 38.68 \text{ kWh}$$

$$\implies Ah_{bat} = \frac{38.68\text{x}10^3}{0.8\text{x}300} = 161.2 \text{ Ah}$$

≈ 180 Ah (commercially available)

2.5.2 Charge Equalisation Circuit

The charge equalisation circuit is an essential component for the battery pack as it can be beneficial when batteries are connected in series to get the desired 300 V. A 300 V battery may not be a readily available resource. Hence, in this study we have considered three 100 V batteries connected in series for achieving the 300 V nominal voltage of the battery pack. The key element towards efficient and economical usage of the battery pack is the employment of charge equalisation circuit. As brought out in [4], the charge equalisation circuit ensures that all the series connected batteries reach the same terminal voltage so that there is no circulating currents between them when applied across load. Similarly, buck-boost converter based

circuit with reserve capacitor bank to equalise the SoC of similar batteries connected in series [5]. Fig. 2.5 depicts the circuit diagram of the CEC employed in the project study. While, many iterative procedures for charge equalisation have been evolved and suggested based on SoC estimation[4]-[6], a simple and cost effective method with simple control strategy has been proposed considering voltage as the ruling criteria for charge equalisation.

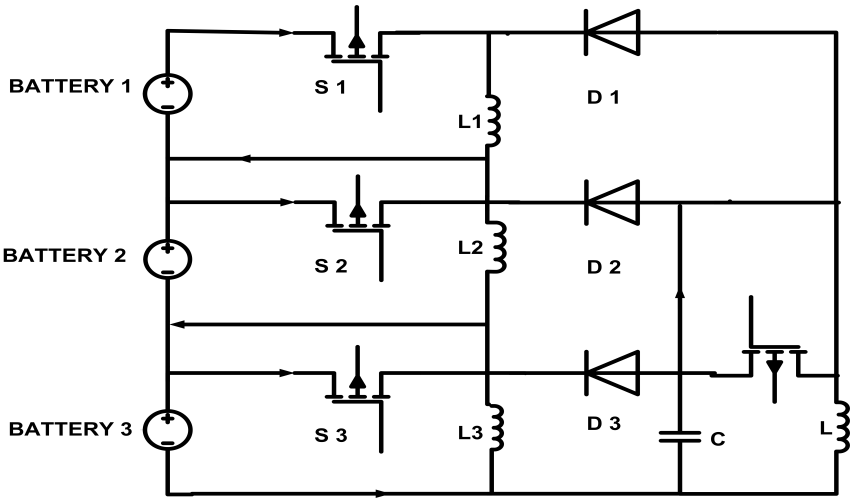

Figure 2.5: Charge equalisation circuit [7], [8]

2.6 Summary

Having discussed the broad overview and the aim of the project in previous chapter, this chapter enumerates the block components of the RMG. Further, the design parameters of PV array are evaluated in detail and taking into account the load curve. A rigorous exercise was undertaken to prepare the load curve from the rating of each appliance and extracting from it the daily peak power demand and energy demand which were found to be 15.24 kW and 125 kWh respectively. The PV array is so designed to cater for the power demand for the daytime as well as during the night. The PV array must be sized to also cultivate the requisite amount energy as demanded by the night time load and store the same in the BESS.

In this study the condition of non insolation days has not been considered, which otherwise shall increase the battery size depending upon the expected number of such days. A PV module/ array is characterised by its short circuit current I_{sc} and the open circuit voltage V_{oc}, which form the ruling criteria for selecting a particular PV module. The required DC link voltage of 500 V and restriction of converters duty not to exceed 0.5, lead the study to consider a PV array with output voltage in the range of 300 V. The main battery bank and secondary battery are rated for

300 V. A charge equalisation circuit has been incorporated in designing the main battery bank, which is assembled using 3 x 100 V batteries in series. This feature enhances the life of the batteries as also contributes to the efficiency of the battery by negating the circulating currents.

Chapter 3

Control Schemes for Converters

3.1 Need for Control

As discussed in Section 2.1, there are three types of converters used in the scheme. Each of them have a defined role which can be implemented by a specific controller choice. The battery and supercapacitor which are operating on bi-directional converters require control scheme for appropriate regulation that decides the buck or boost mode of these converters. These converters also need a suitable controller for ensuring their stable operation using a closed loop control. Similarly, the buck converter also operates on a closed loop control for better transient and steady state performance.

On the other hand, the MPPT controller decides the operating point for the PV array using the incremental conductance algorithm. The application of PV array could be in MPP or off-MPP mode as suggested in some literature [4]. In this case where economy, reduction of size and maximum utilisation of the equipment and resources form the primary objective of the study, MPP operation offers itself as the better choice. In case there be a choice for off MPP operation the scheme could be modified [2]. There are a series of MPPT control techniques which are proven and each of them may suit a different application better over the rest if complexity and economics are also taken into account. While the list is long, an effort has been in the study to summarise them as in following subsections.

3.2 Types of MPPT Techniques

3.2.1 Curve Fitting

In this method a third order polynomial is selected to define Power $P = aV^3 + bV^2 + cV + d$. The coefficients a, b, c and d are determined by sampling of PV voltage and power in intervals. Differentiation of the above mentioned gives

$$\frac{dP}{dV} = 3aV^2 + 2bV + c = 0$$

$$V_{mpp} = \frac{-b + \sqrt{b^2 - 3ac}}{3a}$$

In this technique a, b, c and d are regularly sampled.

3.2.2 Fractional Short-Circuit Current (FSCI) Technique

In the FSCI technique, the nonlinear characteristics of PV system is modeled using mathematical equations or numerical approximations taking account of a wide range of environmental conditions and degradation level of PV panel. Based on those characteristics, a mathematical relation between I_{mp} and I_{sc} is constructed and is linearly depicted by an empirical relation shown below.

$$I_{mp} \approx K_{sc} I_{sc}$$

; where K_{sc} lies in the range of 0.64 - 0.85

3.2.3 Fractional Open-Circuit Voltage (FOCV) Technique

In this technique similar to the previous method, V_{mp} is calculated using the empirical formula

$$V_{mp} \approx K_{oc} V_{oc}$$

K_{oc} can be calculated by analyzing the PV system at wide range of solar radiations and temperatures. In this method, the PV system is open-circuited at load end for a fraction of second and is measured, to calculate V_{mp}. K_{oc} lies in the range of 0.78 - 0.92.

3.2.4 Look up Table

In this technique a wide range of operating voltages, current and power are evaluated at different conditions of temperature and insolation. The data so compiled can be used as a ready reference

for a sensor based algorithm to adjust the operating point to the maximum power point mark.

3.2.5 One Cycle Control (OCC)

This technique employs a single stage inverter where the output current I_{out} can be adjusted according to the voltage of the PV array to obtain the maximum power from it. A single power conversion stage realises the MPPT control as well as a DC-AC conversion.

3.2.6 Differentiation Technique

In this technique, the concept of maxima and minima over the variable of time is made use of wherein,

$$\frac{dP}{dt} = \frac{d(IV)}{dt} = I\frac{dV}{dt} + V\frac{dI}{dt}$$

This technique is measurement intensive and requires a robust controller which may not be economical for certain applications.

3.2.7 Feedback Voltage or Current Technique

This technique is useful for a system without a battery where the aim is to operate the DC link at a fixed voltage using the converter. In this method, the feedback of panel voltage (or current) is taken and compared with a precalculated reference voltage (or current); the duty ratio of DC-DC converter is continuously adjusted so that it operates close to that of MPP.

3.2.8 Feedback Power Variation with Voltage (or Current) Technique

This method is similar to feedback voltage technique except that a feedback of $\frac{dP}{dV}$ or $(\frac{dP}{dI})$ is evaluated every time by varying the voltage(or current) till the desired operating point is tracked where $\frac{dP}{dV}$ or$(\frac{dP}{dI}) = 0$. In this method, power to the load is maximized and not the power from the solar array due to some unavoidable power-loss across the converter.

3.2.9 Perturb and Observe (P & O)

At a given operating point (Ref Fig. 3.1), the voltage and current delivered by the array are measured and corresponding power P_1 is calculated. A small perturbation in duty is given by the controller and the corresponding power P_2 is measured. The algorithm for this technique

evaluates if $P_2 > P_1$ and continues till this condition is reversed or negated. This is the required point of MPP. If however initially itself the perturbation results in $P_2 < P_1$, the duty is altered in the reverse direction.

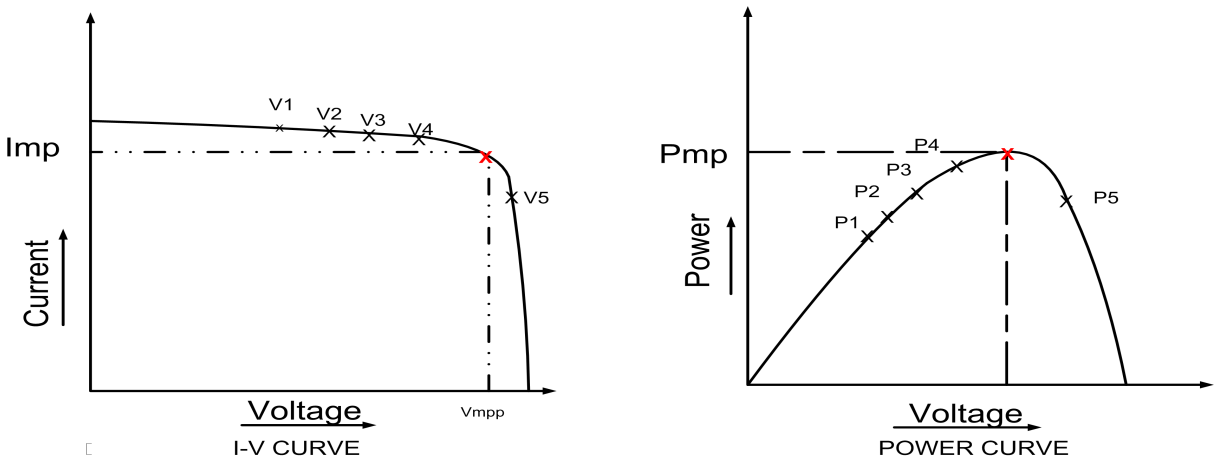

Figure 3.1: MPPT using Perturb and Observe

3.2.10 Incremental Conductance

For a PV system, the derivative of panel output power with its voltage is expressed as

$$\frac{dP}{dV} = \frac{d(IV)}{dV} = I + V\frac{dI}{dV}$$

The solution of the above equation is zero at MPP, positive on the left of the MPP and negative on the right of the MPP (Ref Fig. 3.2). So, the ratio of instantaneous increment of I to instantaneous increment of V is evaluated and compared to the incremental conductance. It is as efficient as P & O and responds quick to atmospheric changes. However, it may require complex circuit. In this study this technique has been employed.

3.2.11 Forced Oscillation Technique

This technique is based on injecting a small-signal sinusoidal perturbation into the switching frequency and comparing the AC component and the average value of the panel terminal voltage as shown in Fig. 3.3. Here, the switching frequency is varied and input voltage is sensed. Scaling down the value of β and comparing βV_i with V_{ref}, the duty cycle of the converter is set at MPP.

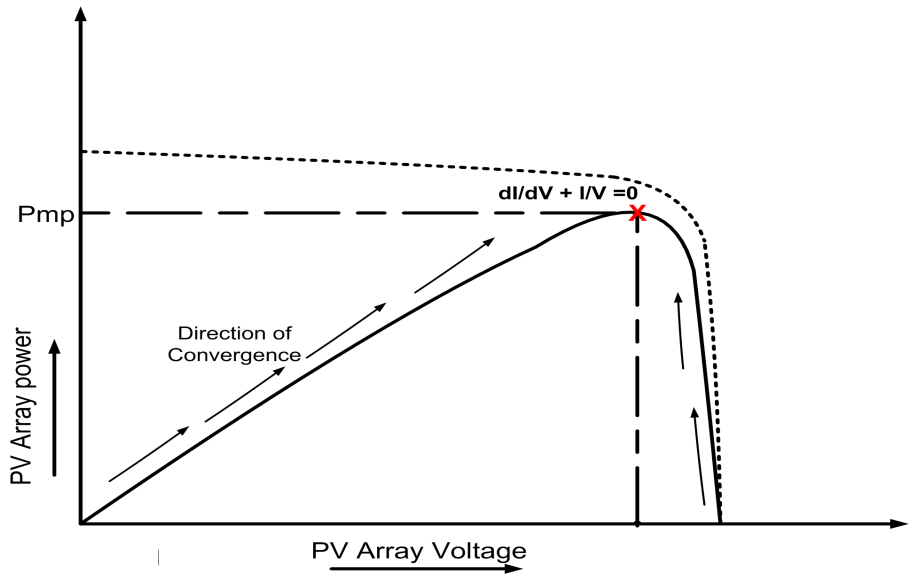

Figure 3.2: MPPT using incremental conductance

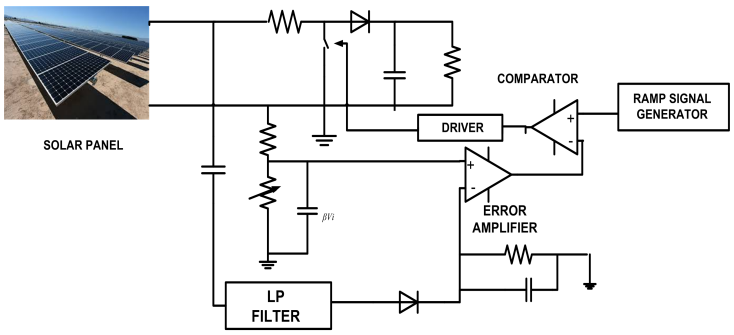

Figure 3.3: Forced oscillation technique

3.2.12 Ripple Correlation Control (RCC) Technique

Connecting a power converter to a PV array generates current and voltage ripples on the PV array. The effect of these ripples is reflected on the power generated by the array. This correlation is used instead of injecting an external perturbation to examine the present operating point and render necessary correction to the duty. The conditions that are examined for ascertaining the MPP are enlisted in following equations.

$$\frac{dv}{dt} \text{ or } \frac{di}{dt} > 0 \text{ and } \frac{dP}{dt} > 0 \qquad \Longrightarrow \text{V} < \text{V}_{mpp} \text{ or } I < I_{mpp}$$

$$\frac{dv}{dt} \text{ or } \frac{di}{dt} < 0 \text{ and } \frac{dP}{dt} < 0 \qquad \Longrightarrow \text{V} > \text{V}_{mpp} \text{ or } I > I_{mpp}$$

3.2.13 Current Sweep Technique

The current sweep technique uses a sweep waveform for the PV array current such that the characteristic of the PV array is obtained and updated at a constant time interval. The V_{mpp} can then be computed from the characteristic curve at the same interval. The function chosen for the current sweep waveform is directly proportional to its derivative as stated below.

$i(t) = k_1 \frac{di}{dt}$

$\implies i(t) = k_2 e^{\frac{t}{k_1}}$

where k_2 is taken as the I_{mpp} at MPP.

Similarly, at MPP the equation $\frac{dP}{dt} = 0$ holds true which can further be written as given below.

$i(t)\frac{dv}{dt} + v(t)\frac{di}{dt} = 0$

Thus, by selecting appropriate the current and voltages can be updated in the given time interval to operate the system at MPP.

3.2.14 Estimated Perturb-Perturb Technique (EPP)

The EPP technique is an extended P & O method. This technique has one estimate mode between two perturb modes. The perturb process conducts the search over the highly nonlinear PV characteristic and the estimate process compensates for the perturb process for irradiance changing conditions. The technique is complex but its tracking speed is faster and more accurate than that of P & O method.

3.2.15 Parasitic Capacitance Technique

Similar to the incremental conductance method, this technique uses the additional affect of parasitic capacitance at the p-n junction of the PV cell. This is incorporated by including the current through the capacitance as $C_p \frac{dV}{dt}$ in the photo current calculated at Eq 2.1

3.2.16 DC Link Capacitor Droop Control Technique

This technique can be applied when the DC link has a inverter feeding a AC grid in parallel. The concept basically utilises the fact that in order to maintain the constant DC link, one must feed as much power as possible into the AC side by increasing the current injected into the inverter, subject to the maximum power the PV array can produce. This happens with the due

support of the AC line which allows the PV to operate at its peak power while any load beyond the capacity of PV is taken care of by the AC system line.

3.2.17 Linearization Based MPPT

This technique uses the fact that the series resistance of the PV cell makes the relation between voltage and current linear. The MPP for a module is evaluated using a set of linear equations for the MPP locus. Though the characteristics of PV module as well as the converters, successive linearisation within a definite range of operation can help design a controller based on this technique.

3.2.18 Intelligence MPPT Techniques

This is a technique which may use fuzzy logic (FL) or artificial neural network (ANN). FL control has fast responses with no overshoot, and less fluctuations in the steady state for rapid temperature and irradiance variations. FL and ANN based MPPT do not require the detail knowledge of the PV module/ array.

3.2.19 Gauss Newton Method

The Gauss-Newton technique is the fastest algorithm, which uses a root-finding algorithm. In its algorithm, first and second derivatives of the change in power are used to estimate the direction and number of iterations of convergence while solving the following equation.

$$v(k+1) = v(k)\frac{\frac{dp}{dv}|v=v(k)}{\frac{d^2p}{d^2v}|v=-v(k)}$$

3.2.20 Steepest-Descent Technique

In this technique, the nearest local MPP can be tracked using a step size corrector $K\epsilon$ as under to the equation in previous sub section. This can be summed up as an equation that follows.

$$v(k+1) = v(k)\frac{\frac{dp}{dv}|v=v(k)}{K\epsilon}$$

3.2.21 Analytic-Based MPPT Technique

This technique is a simple heuristic strategy based on observations and experimental results. This method is based on mean value theorem wherein a ball of small radius is drawn based on

the experimentally obtained values of I_{sc} and V_{oc}.

3.2.22 Hybrid MPPT (HMPPT) Techniques

This technique would use a combination of any of the above techniques in general. To be specific hybrid techniques using both the ANN and P & O were applied. While P & O is simple, accurate and fast, the ANN feature allows the control on step size. Online tracking is possible in hybrid MPPT.

3.2.23 Mismatched MPPT

In practical conditions with large array sizes and huge possibilities of shade on few panels, the need for distributed MPPT is a must which is addressed by this technique.

3.2.24 MPPT Technique for the Project

To exploit the features of speed and accuracy, an incremental conductance technique is employed in the subject study. The logic flow for the same is depicted here:-

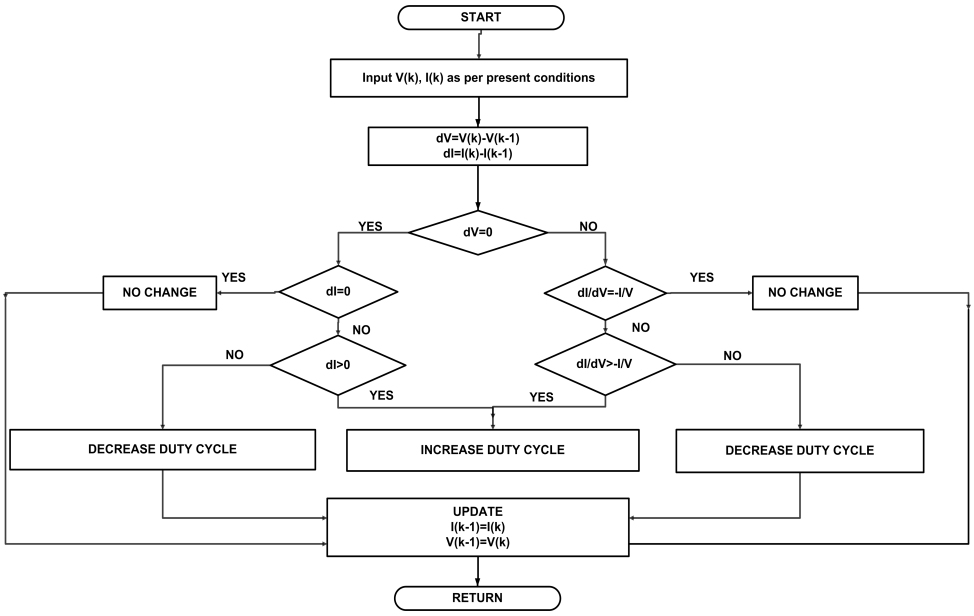

Figure 3.4: Flowchart for incremental conductance

3.3 Design of Controllers for the Project

The proposed design of DC microgrid has automated controls for a variety of requirements. This being an isolated or standalone microgrid does increase the variables manifold. A remarkable example to cite on this account would be the varying insolation throughout the day. Though the design could be more elaborate assuming the non insolation days, however that has not been included in the purview of this project. Apart from this, the varying load brings in more dynamic conditions as in any power system. Overall, it implies maintaining a constant DC voltage of 500 V at the main DC bus which has a varying load (peak load = 15.24 kW) and that of 24 V at DC bus which has a fixed load of 1.089 kW. A total of four DC-DC converters operating in closed loop have been used for the design as stated in subsequent paras with respective controllers for acceptable performance during transients as well as steady state.

3.4 MPPT Controller

A MPPT converter is a boost converter that ensures that the solar array is operating at MPPT. The values of inductance and capacitance are calculated as 1.2 mH and 180 μF respectively using the standard equations for boost converter [5]. The solar array has V_{oc} ranging between 302 V to 312 V as the insolation varies from 200 kW/ m^2 to 1000 kW/ m^2 at 25 degree Celsius. The equations for the transfer function of the boost converter for controlling the input voltage by controlling the duty of the converter is as follows.

$$G_{gd} = \frac{G_{vd}}{G_{vg}}$$

where,

$$G_{vd} = G_{do}\frac{1 - \frac{s}{w_z}}{1 + \frac{s}{Qw_o} + \frac{s^2}{w_z^2}}$$

Similarly ,

$$G_{vg} = G_{go}\frac{1}{1 + \frac{s}{Qw_o} + \frac{s^2}{w_z^2}}$$

Using the above two equations the required transfer function between input voltage and duty is derived in the following manner.

$G_{gd} = \frac{G_{vd}}{G_{vg}}$

$\implies \mathrm{G}_{gd} = \frac{G_{do}}{G_{go}}(1 - \frac{s}{w_z})$

The incremental conductance control as explained in detail at Section 3.1.10 is applied here to estimate the varying maximum power point (MPP).

3.5 Controller for Bi-directional Converter for Battery

The bidirectional converter connected across the battery acts as a two converter allowing power to flow from or to the DC link depending upon whether the solar power is surplus or deficit. This feature allows a flexible operation of the battery to assume the role of source or sink in order to maintain the DC link voltage at 500 V with a ripple variation of not more than 1 %. The converter is controlled keeping in mind the operation as a boost converter of the bi-directional converter which is more likely to drift into an unstable zone on account of the right hand zero of the boost converter for its transfer function for voltage control loop i.e. G_{vd}; hence the application of outer and inner control loop scheme is suggested. The values of inductance and capacitance are calculated as 1.2 mH and $196.1\mu F$ using the standard equations [9].

3.5.1 Modelling of the Current Control Loop

The small signal model for the for the current controller in the inner loop and the voltage controller in the outer loop is given in Fig.3.5. The current loop is supposed to have a response time faster than that of the outer voltage control loop. At the same time, it is expected that the current control loop must have a sampling time greater than that of the modulator that generates the duty for the converter.

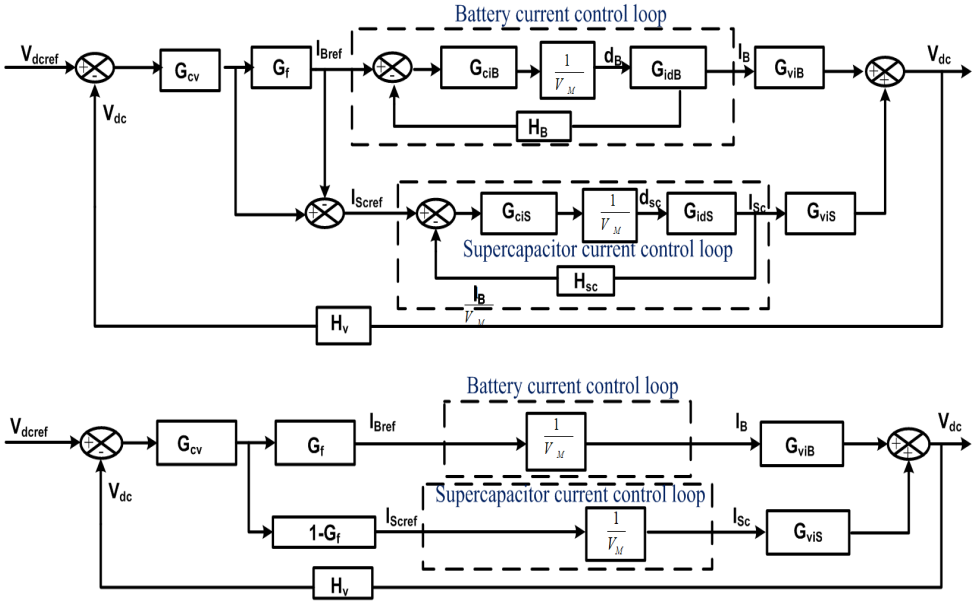

Figure 3.5: Small signal model of the DC Microgrid

The current control loop of the battery is shown in the Fig. **??**. The duty ratio $(\hat{d_B})$ to battery current$(\hat{i_B})$ transfer function $G_{ciB}(s)$ is,

$$G_{idB}(s) = \frac{\hat{i_B}}{\hat{d_B}} = G_{idBo}\frac{1+\frac{s}{w_{ziB}}}{1+\frac{s}{Q_B w_{oB}}+\frac{s^2}{w_o^2}},$$
$$G_{idBo} = \frac{2V_{dc}}{R_L D_B'^2}, w_{ziB} = \frac{2}{R_L C_{dc}},$$
$$Q_B = D_B' R_L \sqrt{\frac{C_{dc}}{L_B}}, w_{oB} = \frac{D_B'}{\sqrt{L_B C_{dc}}}$$

The uncompensated vs compensated Bode plot is at Fig 3.6 with a gain margin (GM) and phase margin (PM) of infinity and 90 degrees. On adding the current controller the the PM and the GM are revised to infinity and 70.3 degrees at $\omega = 1.57e4$ rad/sec.

Figure 3.6: Bode plot for uncompensated and compensated CC for BDC Bat

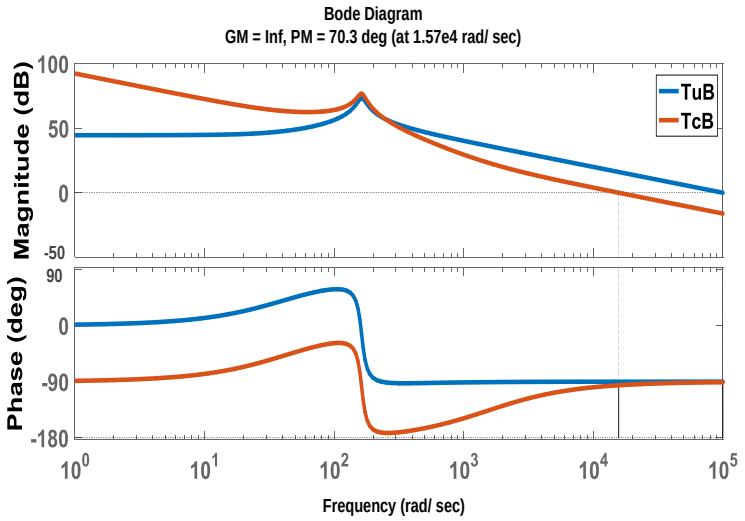

The controller design for the battery current control loop can also be done by adding an inverted zero a decade ahead of the current control bandwidth (w_{cB}). The gain crossover frequency (f_{cB}) is chosen as 2.5 kHz. The inverted zero of the compensator reduces the steady state error of the loop gain by providing high gain at low frequencies. The current controller transfer function is defined by the equation given below.

$$G_{ciB} = G_{ciBo}(1 + \frac{w_{zciB}}{s})$$

where G_{ciBo} is the controller gain at gain crossover frequency.

3.6 Controller for Bi-directional Converter for Super Capacitor

The super capacitor connected to the DC link is a high power density device that acts as important component to absorb the oscillations during the transients. This saves the battery from responding to high frequency transients and shall ensure the longevity of the battery.

Similar to the battery, the super capacitor is also controlled by by an inner current control loop within an external voltage control loop. The Bode plot for the uncompensated bidirectional current control loop is as at Fig. 3.7. The PM and GM are infinite and 90 degrees respectively.

3.6.1 Modelling of the Current Control Loop-SCap

Ref Fig.3.5, the current control loop transfer function $G_{ciS}(s)$ denoting the ratio of super capacitor current $(\hat{i_S})$ to $(\hat{d_S})$ is,

$G_{idS}(s) = \frac{\hat{i_{SC}}}{\hat{d_{SC}}} = \mathbf{G}_{idSo}\frac{1+\frac{s}{w_{ziS}}}{1+\frac{s}{Q_S w_{oS}}+\frac{s^2}{w_{oS}^2}}$,

$G_{idSo} = \frac{2V_{dc}}{R_L D_S'^2}$, $w_{ziS} = \frac{2}{R_L C_{dc}}$,

$Q_S = D_S' R_L\sqrt{\frac{C_{dc}}{L_S}}$, $w_{oS} = \frac{D_S'}{\sqrt{L_S C_{dc}}}$

The controller for the current control loop of the super capacitor is denoted by,

$$G_{ciS} = G_{ciSo}(1 + \frac{w_{zciB}}{s})$$

where the value w_{zcis} is taken a decade ahead of desired current control bandwidth (corresponding to the crossover frequency) for the super capacitor w_{cS}. The considered bandwidth for current control of super capacitor is 2.5 kHz and hence the value of $f_{ciS} = 250$ Hz [4]. The Bode Plots for the uncompensated and compensated current control loops are shown at Fig. 3.7. The GM and PM of the uncompensated loop were infinite and 90 degrees while that of the compensated loop are infinite and 70.3 degrees respectively. The addition of the controller basically increases the DC gain from 45 to 103 which brings the steady state error closer to zero.

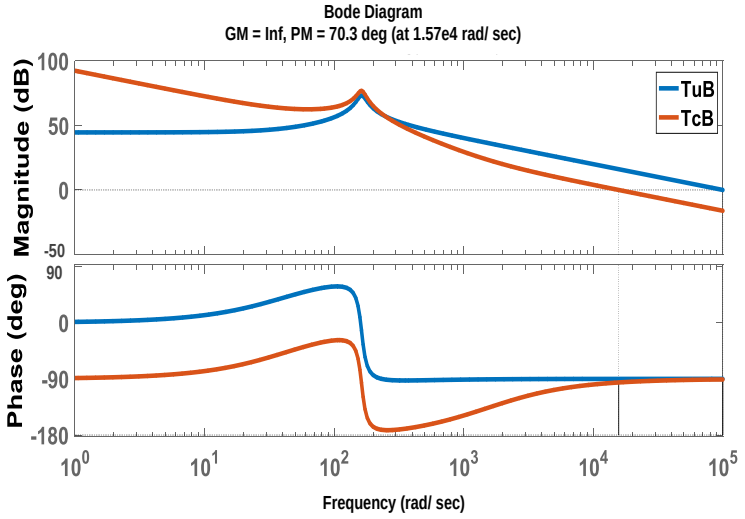

Figure 3.7: Bode plot for uncompensated and compensated CC for BDC Scap

3.7 Voltage Controller Design

The small signal model for the battery and super capacitor is simplified and shown in Fig.3.5. While designing the voltage control loop it is ensured that the battery and super capacitor voltage loop bandwidth is at least $\frac{1}{10}^{th}$ of that current control bandwidths. A low pass filter $G_f(s) = (1 + s\tau_c)^{-}1$, where τ_c is the time constant which designed to get a cut off frequency of 5 Hz. The transfer function of DC link voltage is $G_{cv}(s) = G_{cvo}(1 + \frac{w_{zcv}}{s})$ where w_{zcv} is placed a decade ahead of the desired bandwidth of DC link voltage control loop (w_{cv}). The value of G_{cvo} is selected such that the unity gain crossover of the compensated voltage control loop occurs at w_{cv}.

The frequency response of the uncompensated and compensated voltage loop is given is given at Fig. 3.8 where the PM and DC gain are seen to improve from 91 degrees to 100 degrees and from 13.8 dB to 50 dB. The desired cross over frequency f_{cv} of the voltage control loop is chosen as $\frac{1}{10}^{th}$ of the right side zero frequency of the battery converter, so that its effect in any operating mode is minimum.

Figure 3.8: Bode plot for uncompensated and compensated voltage control loop

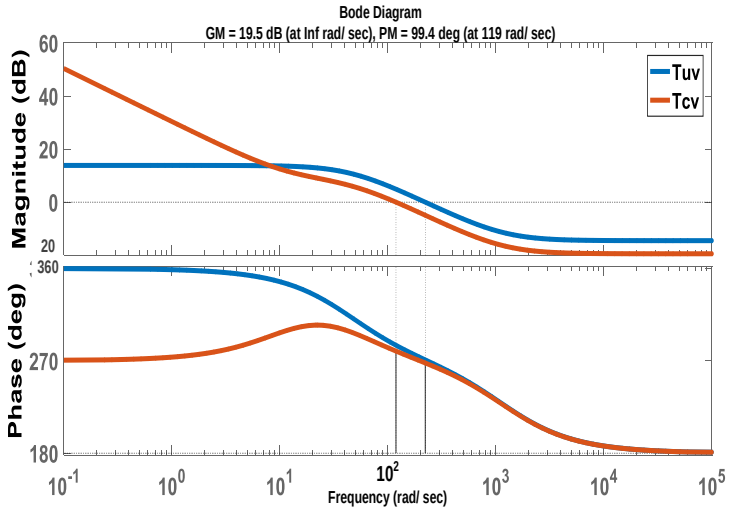

3.8 Controller for Buck Converter

The buck converter is a used in the system to step down the voltage from 500 V to 24 V DC for operating the operational load of LORROS (Long range recce and observation system). The controller is a duty to voltage controller that uses the equations revisited as below [9].

$G_{vd} = \frac{1-\frac{s}{w_z}}{1+\frac{s}{Qw_o}+\frac{s^2}{w_o^2}} = \frac{1}{1+LR+s^2LC}$ where,

$w_z = infinite, w_o = \frac{1}{sqrtLC}$

$Q = R\sqrt{\frac{C}{L}}, G_{do} = \frac{V_o}{D}, G_{go} = D$

The values of L_{buck} and C_{buck} are selected as per the understated equations.

$L_{buck} = \frac{V_o D'}{2\Delta I_L f_s} = 0.393$ mH, $C_{buck} = \frac{\Delta I_L}{8 f_s \Delta V}$ =97μF

where, V = 24 V, I = 29 A, $f_s = 25000$ Hz, D = 0.048

The bode plots for the uncompensated and the compensated buck converter are given at Fig. 3.9, wherein it observed that the PM improves from 6.25 to 61.7 degrees and the DC gain improves from 54 dB to 58 dB.

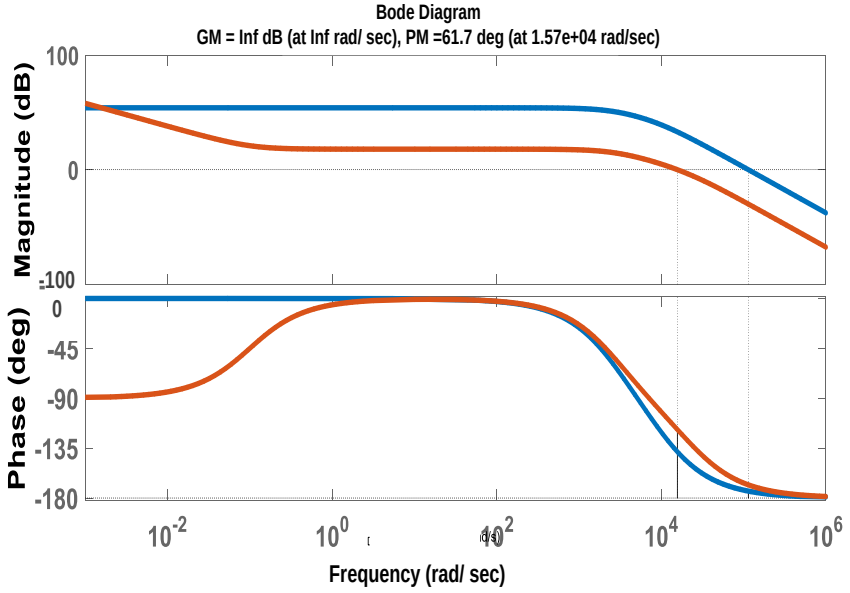

Figure 3.9: Bode plot for uncompensated and compensated voltage control for buck converter

3.9 Control Logic and Strategy

The overall aim of the microgrid is to operate in standalone mode and provide a constant DC voltage of 500 V at the main DC link and 24 V at the secondary DC link. While the load at the main DC link (500 V) is varying, the load at the secondary DC link (24 V) remains constant due the operational load of the surveillance device LORROS operating 24 x 7. The insolation in the Barmer sector is assumed to vary from 200 kW/ m^2 to 1000 kW/ m^2 while the hour equivalent for peak array power Hat_{min} is taken as 5 for the said study.

The control requires the PV array to operate at MPP which is brought to effect by the MPPT controller. This controller shall be operating to give a PV output voltage in the range of 300-315 V with varying temperature and insolation. The logic of incremental conductance has been

applied which has been discussed in detail in Section 3.2.

The bidirectional converter for the battery has an important role to operate in the required mode to maintain the DC link voltage of 500 V. For excess power being generated the converter is required to operate as a buck converter and allow power flow to the battery which in this circumstance is operating as a sink. On the contrary, when the power generated from the PV is deficit compared to the load demand, the battery is required to operate as a source. For the battery operating as a source the bi directional converter operates in the boost mode when it steps up the voltage from 300 V to 500 V.

The logic for identifying the mode of operation for the battery is generated by computing the value of I_{Bnet} which is extracted using a low pass filter from the I_{net} to be supplied to the DC link. The current I_{Bnet} will be positive during the deficit power mode and negative during the excess power mode of operation. I_{net} is actually the net current required to be supplied from the battery and super capacitor combination to the DC link. The existence of super capacitor is primarily to absorb the high frequency transients that may be detrimental to the battery. Hence, the super capacitor reference current I_{Sref} shall always have the component I_{osc} to account for the oscillating components. It may have an addition component when it's state of charge (SoC) falls below the lower limit 0.9 to allow the battery to pump the required amount of charge to the super capacitor.

Apart from this there is additional control considered in the study which basically utilises as secondary battery bank to negotiate unforeseen situations. In this case a secondary battery of 300 V and 180 Ah has been considered to operate in case the main battery bank fails to absorb the excess power once it reach the upper limit of SoC (BH) or to pump the additional power sought from the main battery when it has reached the lower level of battery SoC (BL). In either cases a logic gate is operated to check the SoC level of the main battery. The exact capacity of the secondary battery may also be a considered by the user if the applied situation is expected during operation e.g continuous days of non insolation days. This has not been considered in this project. This logic enables us to design a smaller main battery, while the spare battery takes over the role of main battery during non autonomous days or unforeseen situations. The spare battery may otherwise be applied for less critical tasks and always has sufficient capacity to charge or discharge. The flow chart Fig. 3.10 represents the logic flow for the generation of I_{Bref} and I_{Sref}.

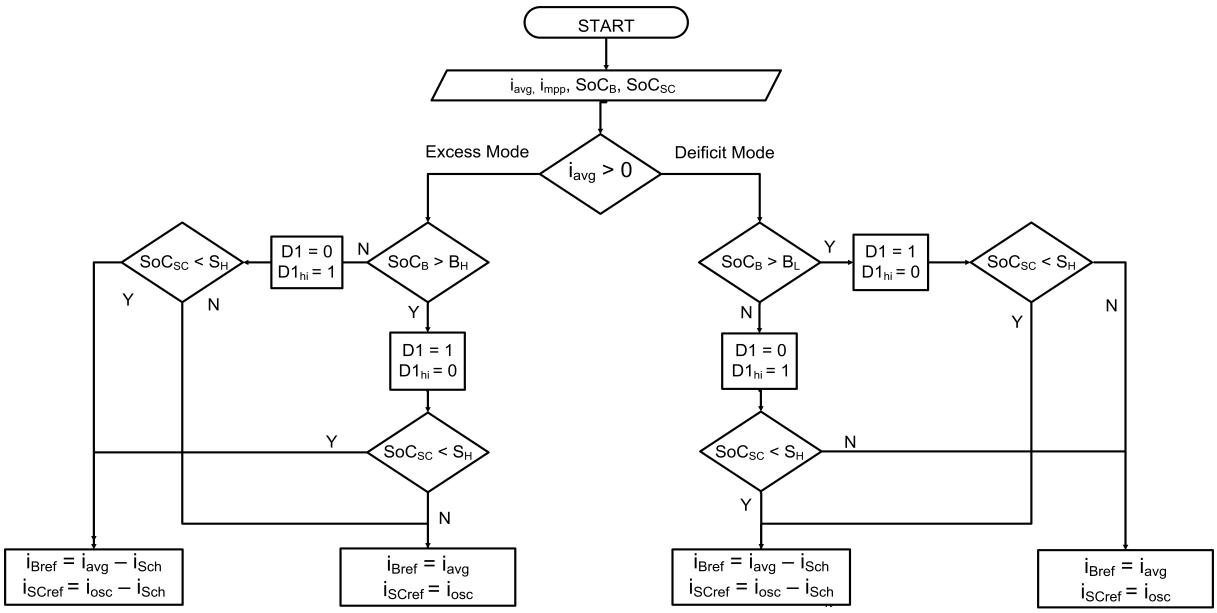

Figure 3.10: Flowchart depicting the logic flow for generation of references

3.10 Summary

This chapter has the essence of the project study in terms of design of controllers. The MPPT controller uses the efficient method of incremental conductance to facilitate the operation of PV converter at MPP. This ensures complete utilisation of the PV panel and resources as required in any military application. The bidirectional converters are governed by two sets of control schemes. While the PI controller ensures the desired closed loop operation for these converters, the control logic for deficit/ excess PV power generates the reference currents I_{Bref} and I_{Sref} for the bidirectional converters. The buck converter uses a simple lead compensator and PI controller for the said operation.

Chapter 4

Simulation and Results

In this chapter, a detailed simulation study has been carried out to examine the operation of the RMG in various modes and in varying conditions of insolation temperature, battery SoC and supercapacitor SoC. The variation in load has also been considered as a simulated input in the form of load curve. The system parameters evaluated in the preceding chapters are enumerated in Table 4.1. The PV array based relocatable microgrid can be operated in different modes depending upon the insolation, load and the SoC. The controlled bi-directional converters play an important role while operating in the selected mode. The control logic evaluates the PV power available and compares the same with load demand using the voltage and current control loops. A variety of control logic are available for implementing the operation, however this study has been restricted to simple linear control using PI control and hysteresis control.

In this project the battery bank has been restricted to a capacity assuming there is no day of autonomous operation. Yet the requirement for maintenance in battery bank can not be ruled out. This may need a secondary battery bank of a possibly lower capacity. The control logic in the study enables the secondary battery in case the SoC of the main battery violates the upper or the lower limit.

4.1 Deficit Power/ Main Battery Discharging Mode

The system shall be operating in this mode whenever the insolation is lesser than what is required to maintain the DC link with PV power exclusively. The logic control closes the switch S1 to ON position and opens the switch S2 to OFF position. The power from PV array is either zero or inadequate for the load as indicated by the dotted line. The power flow diagram for the

circuit is shown in Fig. 4.1

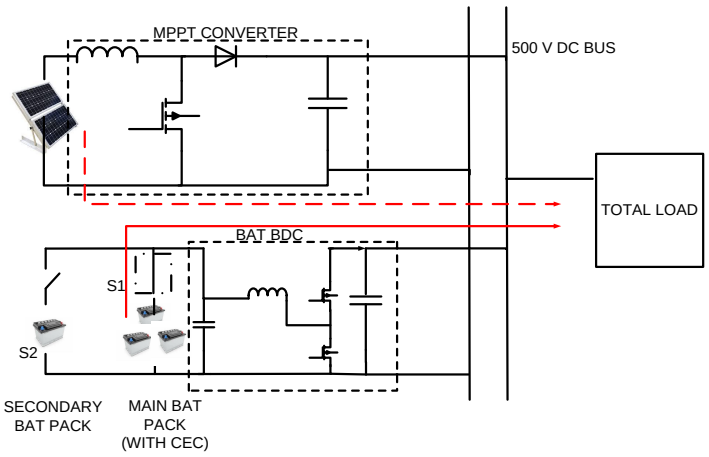

Figure 4.1: RMG operation in Mode I (a)

4.2 Deficit Power/ Secondary Battery Discharging Mode

The operation in this mode is similar to the previous mode except that the main battery would have disconnected automatically through the operation of a switch/ relay (S1) while the secondary battery shall connect automatically to start supplying the required power to the DC link as depicted in the following diagram.

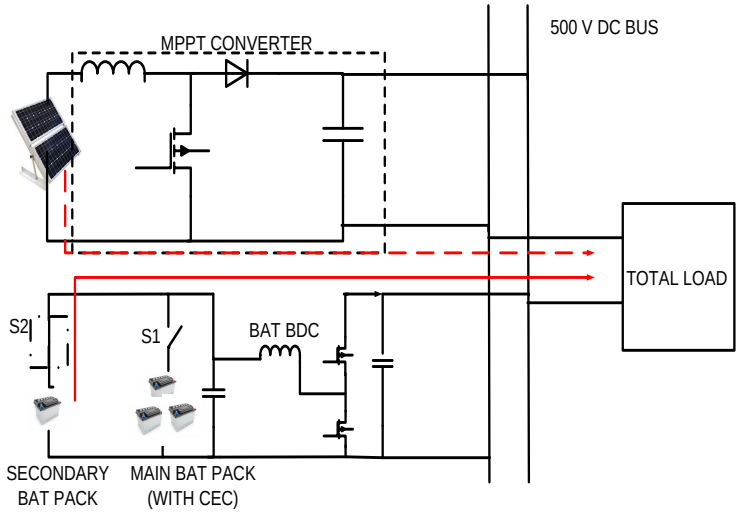

Figure 4.2: RMG operation in Mode I (b)

4.3 Excessive Power/ Main Battery Charging Mode

The system shall be operating in this mode whenever the insolation is greater than what is required to maintain the DC link with PV power exclusively. In such a case the battery shall be operating as sink and the battery converter shall operate in the buck mode. The supplementary battery in this mode shall continue to operate for its primary application, which could be a charging set for wireless communication handsets, GPS etc. The power flow diagram for the circuit is shown below.

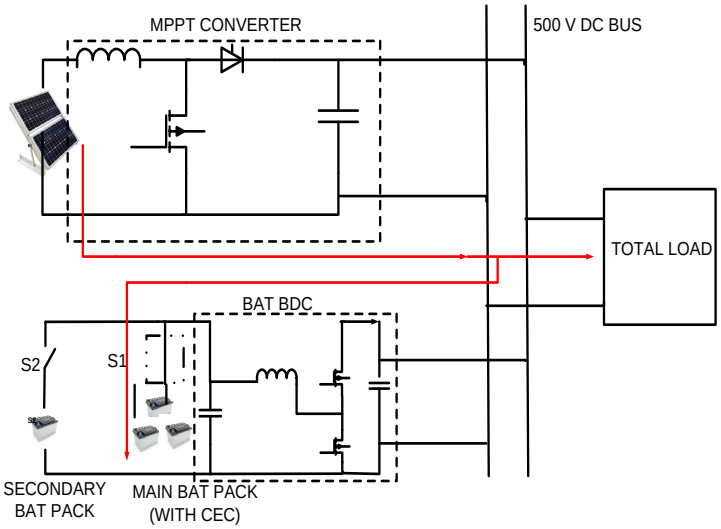

Figure 4.3: RMG operation in Mode II (a)

4.4 Excess Power/ Secondary Battery Charging Mode

Similar to the operation of secondary battery in Mode II, here the secondary battery shall connect to the system while the main battery being fully charged shall disconnect from the system. Fig.4.4 shows the power flow and the simulation results for this mode. The secondary or supplementary battery may have a primary role for another application, however based on the logic circuit command from the RMG it is designed to switch to the RMG and take over the role of the main battery bank of the RMG. This saves the effort and economy of expenditure towards a dedicated additional capacity for the RMG.

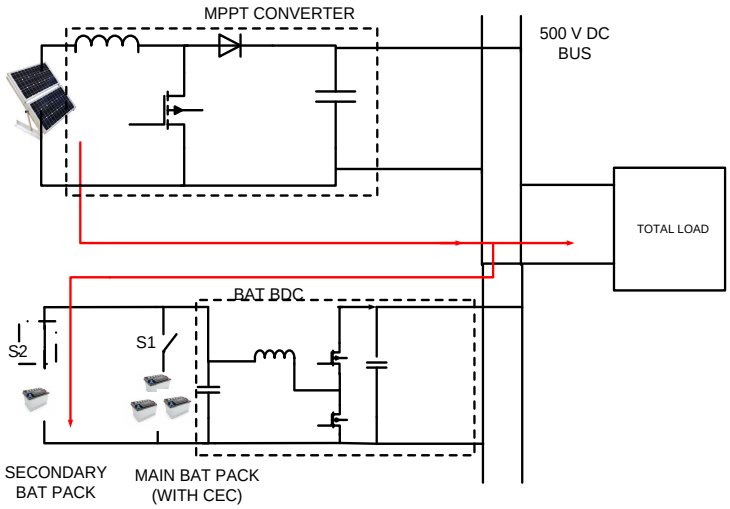

Figure 4.4: RMG operation in Mode II (b)

4.5 Charge Equalisation Circuit

As brought out in Chapter 2, the charge equalisation circuit used in the study enables equally balanced SoC levels in all the batteries prior to the setup or operation of the RMG. This ensures no circulating currents between the batteries and enhances the life of the batteries[3]. It can be observed from the simulation result in Fig.4.5 that the voltages of the three batteries connected in series converges to 101.3 V at t = 50, which initially at t=0 were 99.5 V, 101.1 V and 101.8 V for battery 1, 2 and 3 respectively.

Figure 4.5: Charge equalization circuit output

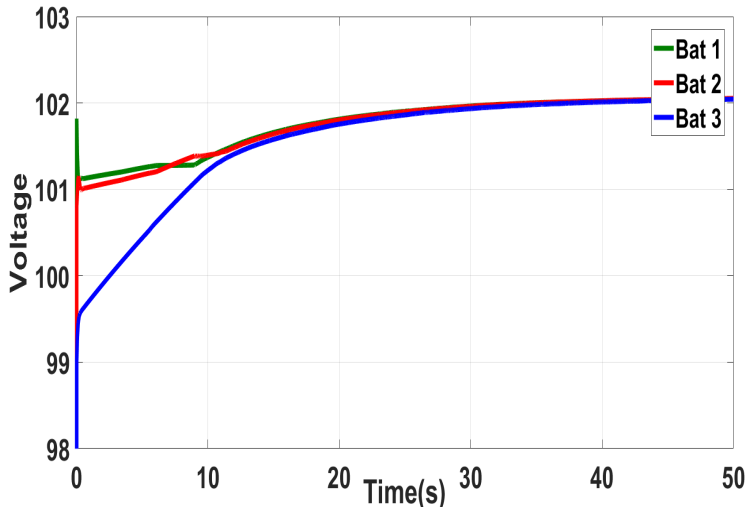

4.6 Simulink Results and Discussion

4.6.1 Ambient Conditions Variation

The variation of PV voltage and current is expected in adherence to the characteristic IV curve of the array as in Figs. 4.8 and 4.9. While the increase in insolation tends to increase the operating voltage logarithmically due to positive insolation coefficient, any increase in temperature shall decrease the voltage owing to negative temperature coefficient for PV voltage. In this study a mono crystalline PV array is considered that has a higher absorption index in comparison to the poly crystalline modules. A recent development in the field of PV modules has found PV arrays which capture solar energy on either surfaces.

The net effect causes the voltage from PV array to vary in the approximate range of 288 V to 301 V, during the entire day. The PV voltage and current are depicted in Fig. 4.10. It is observed that during the non insolation period 1900 hr to 0700 hr of the next day, the PV is generating zero power as PV voltage and currents continue to be zero. However, with the sunrise when the insolation is 200KW/ m^2 it reaches a voltage V_{mpp} of 302 V and continues to decrease with MPPT control as the temperature increases. The variation of insolation and temperature considered for the general area of Barmer are represented as in Figs.4.6 and 4.7.

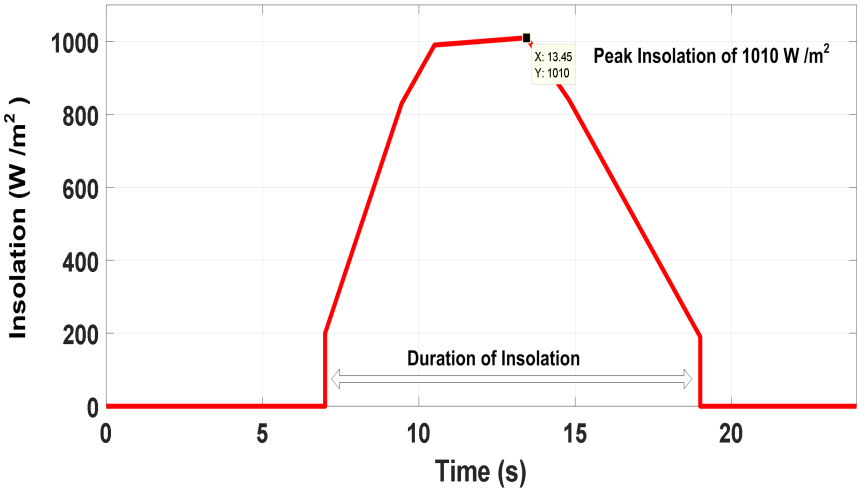

Figure 4.6: Variation in insolation in 24 hr cycle

.

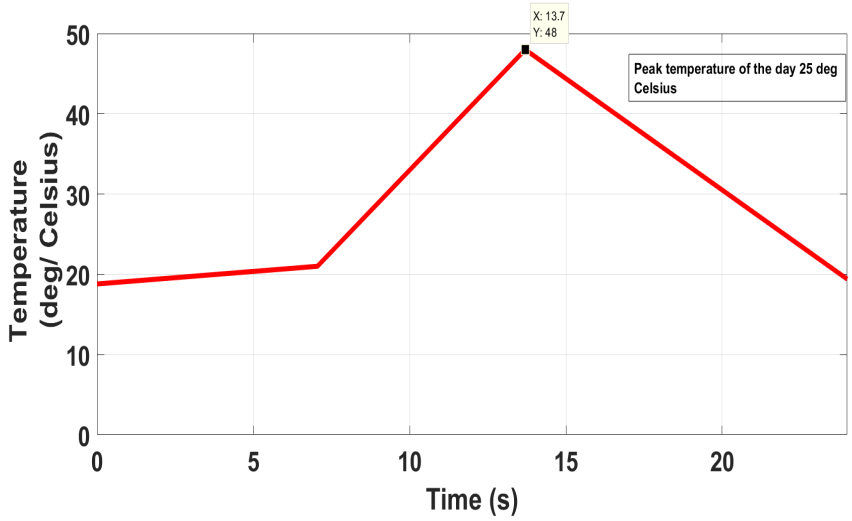

Figure 4.7: Variation in temperature in 24 hr cycle

4.6.2 Response of PV Array to Insolation and Temperature

A PV panel as explained at Section 2.1, is combination of several PV cells connected in parallel and series to serve a predetermined range of load. The IV curve characteristics of any PV array on study reveals that insolation and temperature have a major bearing on the PV output. It is observed that as the insolation increases the I_{SC} increases rapidly while the V_{oc} increases logarithmically. The insolation coefficient for voltage and current are positive and hence the power output increases as the insolation increases. On the other hand temperature has a negative effect on the voltage and power output of the PV array. This is because of negative temperature coefficients ($\beta = -0.350\%$/ degree Celsius) and $\gamma = -0.450\%$/ degree Celsius of the array. The same is depicted in Figs. 4.6 and 4.9

4.6.3 PV Array Output with MPPT

The results obtained from simulink are analysed in this section. The variation in insolation, temperature, battery SoC, supercapacitor SoC and load have been factored in to find out the expected results.

4.6.4 Battery and Supercapacitor SoC

The SoC of the battery shall also vary through the day as the battery discharges during the off insolation hours and again it starts charging during the insolation hours. It is observed that the battery current increases upto an average value of 20 A during discharging and upto a 50 A

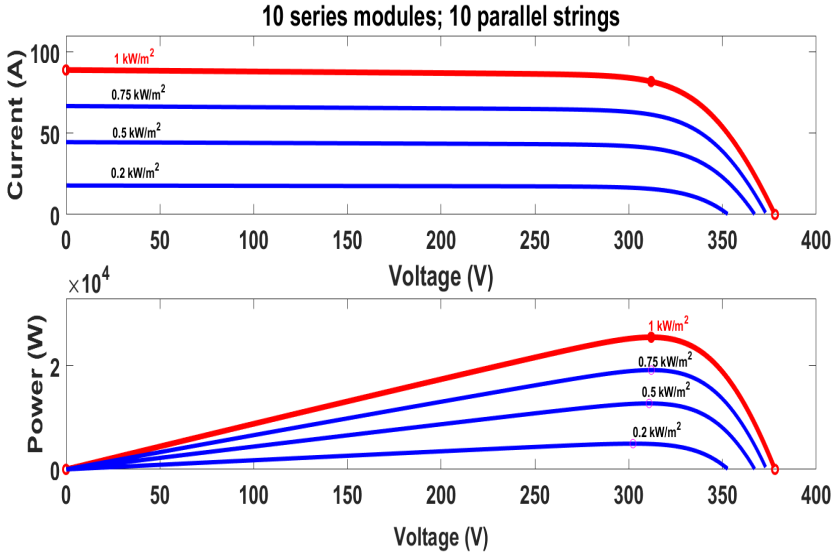

Figure 4.8: PV array response to insolation variation

while charging. For this reason the 540 Ah battery is designed for a C_{10} rating. The plot at 4.11 depicts the variation in 24 hr that has been considered for the battery and supercapacitor to define the four possible modes considered for the study. The duty for the two batteries are complimentary in nature as the second battery comes into play only if the main battery is saturated or is undercharged as represented in Fig. 4.11.

4.6.5 Duty of Main and Secondary Battery

As explained in Section 2.3 the main battery is designed to operate as a buffer for the PV system. However, a situation may arise wherein the main battery may not be able to charge owing to saturation or discharge due to over discharging. For that circumstance, depending upon the likely duration of the calamity or expected ambient conditions of weather one may design a bigger battery size, which however may be uneconomical as that additional capacity shall be unused for most of the time. As a solution to this what has been considered is a unique logic where in another battery which serves a lesser critical load of similar voltage rating shall come into play and take over the duties of the main battery automatically. This shall result in adequate cost cutting. The variation in duty and the complimentary operation of the two batteries is depicted in Fig.4.12

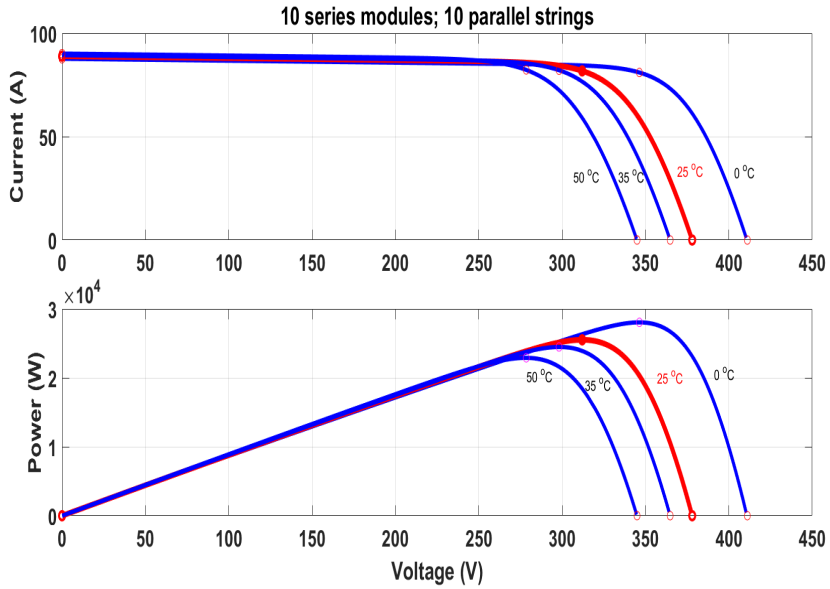

Figure 4.9: PV array response to temperature variation

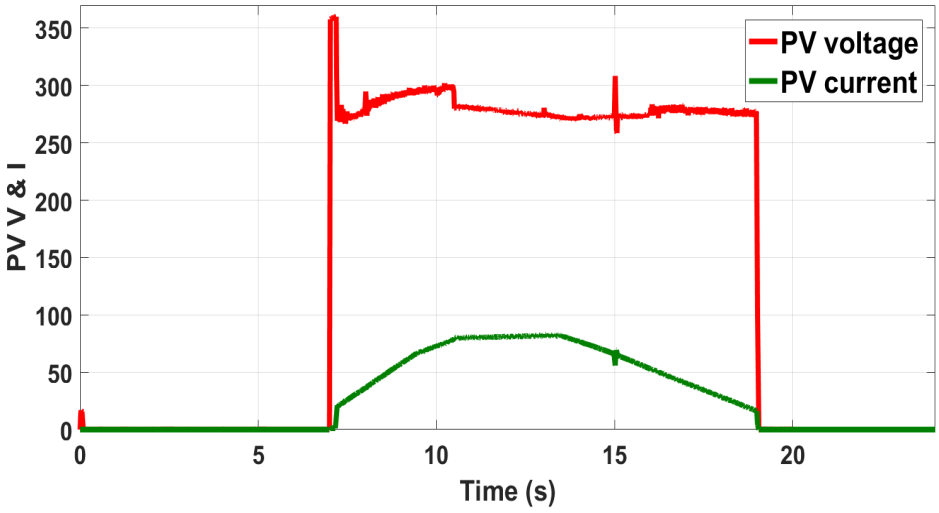

Figure 4.10: PV array output with incremental conductance MPPT

4.6.6 Battery Current in Various Modes

The batterys shall charge or discharge based on insolation available to the PV array, the instantaneous power demand from the load and the SoC of the battery . A logic to this effect has been implemented in this study to allow automatic switching of the modes ensuring an uninterrupted supply and to ensure best utilisation of the solar power. The automatic charging and discharging has been exhibited in the plot in Fig.4.13

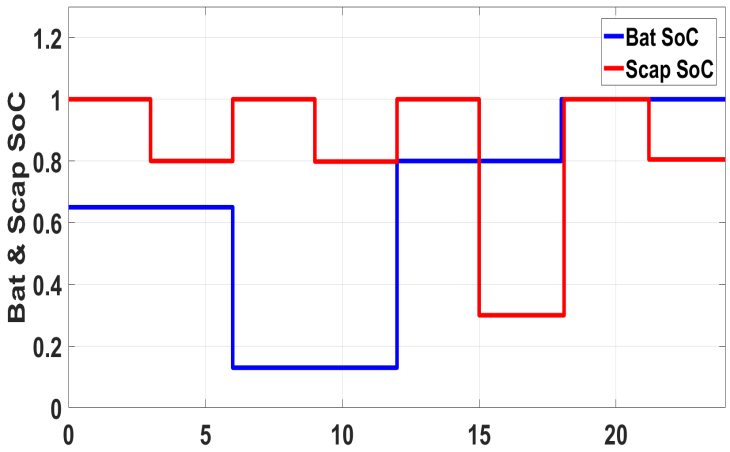

Figure 4.11: SoC of battery and supercapacitor

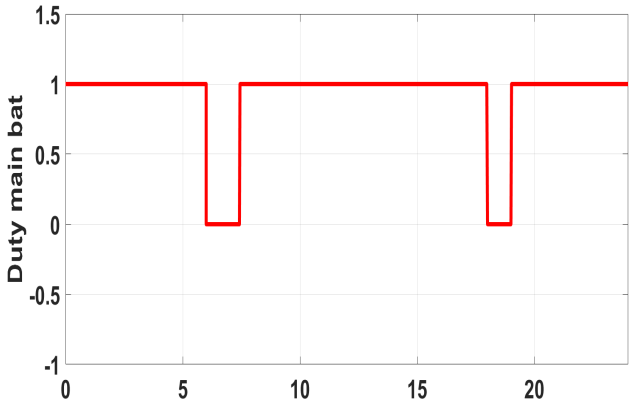

(a) Main battery duty

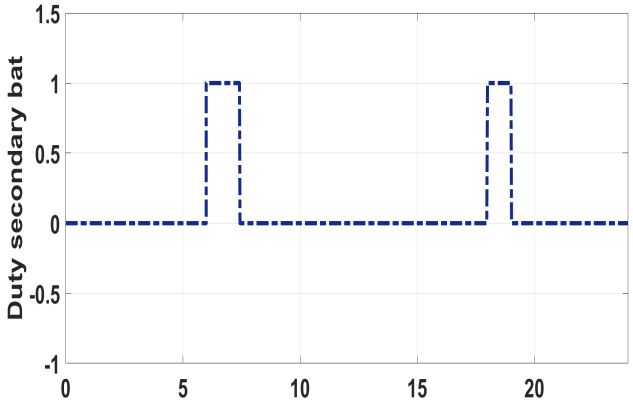

(b) Secondary battery duty

Figure 4.12: Battery duties based on their SoC and PV power

4.6.7 DC Link Voltages and Current

The DC link voltage at the main bus is required to be maintained at 500 V. The battery bank in conjunct with the PV array and the super capacitor does the same using the logic used in the

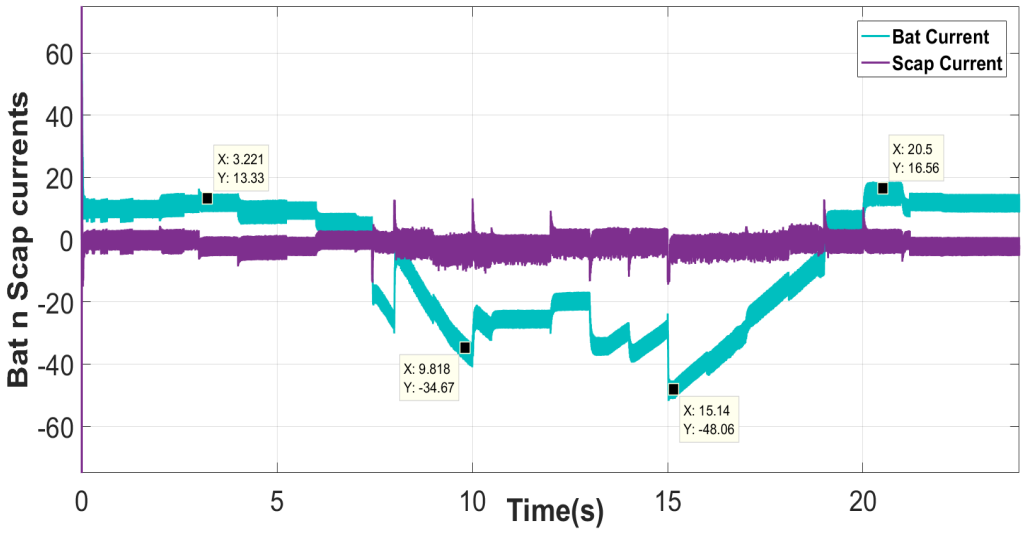

Figure 4.13: Battery and Scap currents

system. Whenever there is a change in insolation or load that causes a difference in the power demand and PV power, the DC link voltage is likely to fall or rise depending on whether there is deficit power or excess power from the PV array. As a buffer the battery provides the power to the load at the DC link or otherwise absorbs the excess power from PV to maintain the DC link voltage. The super capacitor absorbs the frequency oscillations that may damage the battery in its absence. Voltage spikes are observed at 0700hr, 0800hr,1300hr, 1500hr owing to sudden change in insolation and switching of loads. The voltage and current at the 500 V DC link is given the plot at Fig.4.14

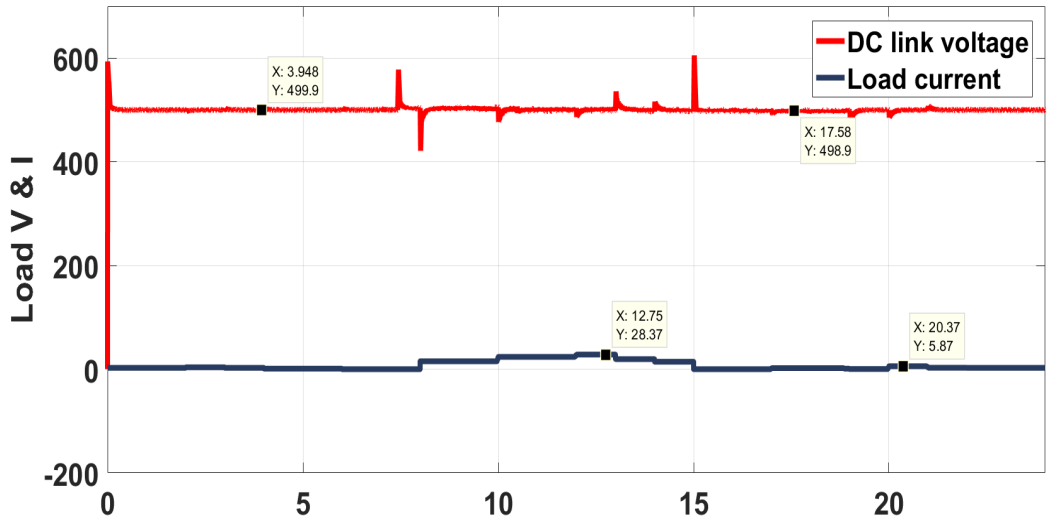

Figure 4.14: Main DC link voltage and load current

4.7 Summary

The results of simulation clearly exhibit the efficacy of the designed PV RMG. The variation in insolation and temperature during the daytime is effectively sensed by the MPPT controller to regulate the PV output, thus maintaining the PV voltage in the range of 288 V-306 V. The BDC of the battery bank and the supercapacitor ensure the injection of current into the DC link as directed by the control scheme. The supercapacitor is observed to absorb the spikes in voltages which would otherwise have been detrimental to the battery life. The battery bank is so designed that it has adequate capacity 300 V, 540 Ah for the night time load i.e. 27.08 kWh while it charges up during the period of insolation without exceeding the C rating limits. In case for unforeseen situations or for maintenance the secondary battrey can take over from the main battery for a limited period. The DC link voltage is maintained at 500 V with a ripple not exceeding 1%. The load current is also regulated accordingly and ripple is limited to 10%.

4.8 System Parameters

The system parameters considered or evaluated during the course of the project study for the PV array, battery bank, supercapacitor and converters are enumerated in the table as follows.

Table 4.1: System parameters for RMG

Sno	Parameter	Symbol	Value
1.	Peak power demand	W_{peak}	15. 24 kW
2.	Daytime energy demand	Wh_{day}	85. 193 kWh
	Ni time energy demand	Wh_{ni}	27.08 kWh
3.	PV module V_{oc}	V_{oc}	37.8 V
	PV module I_{sc}	I_{sc}	8.89 A
4.	MPPT converter Inductance &	L_{mppt}	1.2 mH
	Capacitance	C_{mppt}	185 μF
6	BDC Inductance &	L_b	1.2 mH
	Capacitance	C_b	195 μF
8.	Buck Converter Inductance &	L_{buck}	394 H
	Capacitance	C_{buck}	97μF
9.	Battery Bank voltage rating	V_{bat}	300 V
	Ampere Hr rating	Ah_{bat}	540 Ah
10.	Super capacitor capacitance	C_{sc}	84 F

Chapter 5

Conclusion and Scope for Future Enhancement

5.1 A Brief Summary on the Project Endeavour

The said study has been carried with real possible loads, load patterns, insolation data for an actual region (Barmer), specifications of commercially available PV modules and a possible scenario of deployment for exercise or operations. There is distinct load that has been shown as operational (critical) load which is bound to exist for any unit /HQ deployed and the other being the varying load. For reconnaissance and surveillance units the critical load could be even higher and characterised by a limited or absence of varying load. The scheme may see variation in topology or logic accordingly, however the concept may continue to be the same. The PV arrays can be used as the roof tops of the ALS or TATRA vehicles and all such vehicles that may be planned to be a part of the RMG must be modified by the manufacturer. This shall enable capturing the energy while on move as well. The battery bank suggested needs to be tailor made; in other words a standardisation may be needed to be carried out to group certain kinds of applications under single head for the ease of bulk manufacturing, economy and inter-operability of the batteries. As on date the 12 V or 24 V batteries could be combined using the charge equalisation circuit or the voltage balancing circuit for obtaining a possibly smaller DC link voltage like 48 V .

5.2 Application of Inverter and Grid Synchronisation

A step beyond this project could be possibly enhanced with a controlled inverter for serving the varying AC load instead of the DC load considered on the 500 V DC link. That would be more prudent and practical in the scenario where the laods are still AC loads. In the same direction grid synchronisation using droop control could be a further scope for the study. This shall eliminate the dependence on batterys for applications when the deployment is not in isolated areas or enemy areas [9],[10].

Overall this is a workable system and much can be done to amalgamate various power source. An idea of including diesel generators (DG) as in [12] could be considered as a supplementary power source to the PV. The PV in a full fledged way may take time to be incorporated as a reliable source for operations. Meanwhile such an arrangement with DG could be phased solution to the subject of mobile power source in military applications.

Bibliography

[1] Paul D; Robert M; Triew M; Greg B; Easan D; Mauren H; Matthew M;"Solar Power as a major contributor to the US Grid", IEEE Power and Energy Magazine, vol 22, Apr 2013.

[2] Bidyadhar Subudhi ; Raseswari Pradhan,A Comparative Study on Maximum Power Point Tracking Techniques for Photovoltaic Power Systems, IEEE Transactions on Sustainable Energy Year: 2013, Volume: 4, Issue:1

[3] Design and small signal analysis of DC microgrid with hybrid energy storage system Srikanth Kotra ; Mahesh K. Mishra ; Nakka Pruthvi Chaithanya

[4] 2017 IEEE PES Asia-Pacific Power and Energy Engineering Conference (APPEEC) Year: 2017 Robert W. Erickson - FUNDAMENTALS OF POWER ELECTRONICS (1997, Springer)

[5] On the Perturb-and-Observe and Incremental Conductance MPPT Methods for PV Systems Dezso Sera ; Laszlo Mathe ; Tamas Kerekes ; Sergiu Viorel Spataru ; Remus Teodorescu IEEE Journal of Photovoltaics Year: 2013 , Volume: 3 , Issue: 3

[6] Hotspots of solar potential in India T V Ramachandra1,2,3,* Rishabh Jain1 Gautham Krishnadas1 http://wgbis.ces.iisc.ernet.in/energy/ 1 Energy Wetlands Research Group, Center for Ecological Sciences [CES], 2 Centre for Sustainable Technologies (astra), 3 Centre for infrastructure, Sustainable Transportation and Urban Planning [CiSTUP], Indian Institute of Science, Bangalore, Karnataka, 560 012, India

[7] L Umanand,IISC, Bengaluru,"Design of Photo voltaic systems course" https://nptel.ac.in/courses/117108141/

[8] Dynamic charge equalisation for series-connected batteries C.S. Moo ; Y.C. Hsieh ; I.S. Tsai ; J.C. Cheng IEE Proceedings - Electric Power Applications Year: 2003 , Volume: 150, Issue: 5

[9] Sina Parhizi ; Hossein Lotfi ; Amin Khodaei ; Shay Bahramirad, "State of the Art in Research on Microgrids: A Review" IEEE Access Year: 2015 , Volume: 3

[10] J.A.P. Lopes ; C.L. Moreira ; A.G. Madureira, "Defining control strategies for MicroGrids islanded operation" IEEE Transactions on Power Systems Year: 2006 , Volume: 21 , Issue: 2 Octavian Cornea ; Gheorghe-Daniel Andreescu ; Nicolae Muntean ; Dan Hulea, "Bidirectional Power Flow Control in a DC Microgrid Through a Switched-Capacitor Cell Hybrid DCâĂŞDC Converter IEEE Transactions on Industrial Electronics Year": 2017 , Volume: 64 , Issue: 4

[11] Optimal operation of PV-DG-battery based microgrid with power quality conditioner Shatakshi Jha ; Ikhlaq Hussain ; Bhim Singh ; Sukumar Mishra

IET Renewable Power Generation Year: 2019 , Volume: 13 , Issue: 3 Pages: 418 - 426